



Performance of various water-based fire suppression systems in tunnels with longitudinal ventilation

Ying Zhen Li^{a,*}, Haukur Ingason^a, Magnus Arvidson^a, Michael Försth^{a,b}

^a Safety and Transport - Fire and Safety, RISE Research Institutes of Sweden, Borås, Sweden

^b Structural and Fire Engineering, Luleå University of Technology, Luleå, Sweden

ARTICLE INFO

Keywords:

Tunnel fire
Fire suppression
Heat release rate
Water density
Operating pressure

ABSTRACT

Low pressure, medium pressure and high pressure water-based fire suppression systems were tested in a medium scale tunnel (scale 1:3). The primary objective was to investigate which of these systems are most effective in the suppression or control of different types of tunnel fires. The default low, medium and high pressure systems refer to full scale water flow rates of 10 mm/min, 6.8 mm/min and 3.7 mm/min, respectively. Some other water densities were also tested to investigate the effects, as well as different ventilation velocities and activation criteria. Several series of fire tests were conducted for different fire scenarios. The fire scenarios considered included idle wood pallet fires, loosely packed wood crib fires, loosely packed wood and plastic crib fires, and pool fires, with or without a top cover on the fuel load. Comparisons of the three default systems based on the three parameters: heat release rate, energy released and possibility of fire spread, show that the performance of the default low pressure system is usually the most effective based on the parameters studied. The default high pressure system usually yields results less effective in comparison to the default low pressure system. The performance of the default medium pressure system usually lies in between them. The high pressure system behaves very differently in comparison to the others, in terms of tunnel ventilation velocity, water density, operating pressure, and the presence of the top cover.

1. Introduction

To meet the increasing needs of fast transportation, tunnels and underground structures are being built worldwide. Examples in Sweden are the North Link in Stockholm (opened in 2014) and the planned Stockholm Bypass (to be completed in 2034). Meanwhile, numerous catastrophic tunnel fires have occurred over the past decades, causing huge life and economic losses. For example, in the Mont Blanc tunnel in 1999, 34 vehicles caught fire, resulting in 39 deaths, 900 m long severely damaged structure and 3 years' closure [1].

The need to improve tunnel fire safety levels is recognized by international organizations and authorities and the use of water-based fire suppression systems or Fixed Fire Fighting System (FFFS) in road tunnels attracts much interest. As an example, the Swedish Transport Administration has planned to use FFFS for the Stockholm Bypass and also for upgrading old road tunnels in Sweden [2]. In the past two decades, there have been numerous large scale fire tests conducted with FFFS, mainly to validate the performance of FFFSs prior to their installations in real tunnels [3]. Li and Ingason [4] gave a summary of previous large-scale

tunnel fire suppression tests. These tests include the Second Benelux Tunnel tests [5], the IF tunnel tests in the UPTUN project during 2002 and 2004 [6], the IF tunnel tests by Marioff Corporation Oy in 2004 [7], the Hagerbach tests carried out in 2005 by Mawhinney [8] and Tuomissaari [7], the San Pedro de Anes tunnel tests by Marioff Corporation Oy in 2006 [7,8], the Runehammar tunnel tests by SINTEF & Efectis Nederland BV during December 2007 and January 2008 [9], the San Pedro de Anes tunnel fire tests conducted in the SOLIT project in 2008 [10], and the SOLIT2 project during 2011 and 2012 [11], the San Pedro de Anes tunnel tests by LTA Singapore in 2011 [12,13], and the Runehammar tunnel fire tests by Ingason et al., in 2013 [14]. Although these large scale tests varied in scope and performance, they have contributed to improving the knowledge on suppression efficiency of FFFS. Since then there have been some additional large scale fire tests, e.g., the Runehammar tunnel fire tests comparing the performance of different large droplet nozzles by Ingason et al., in 2016 [3], the heptane pool fire tests by Chang et al. [15], the diesel pool fire tests by Li et al. [16], and the high pressure water mist tests in the Runehammar tunnel by Lei et al., in 2021 [17]. There have also been model-scale tunnel fire tests

* Corresponding author.

E-mail address: yingzhen.li@ri.se (Y.Z. Li).

<https://doi.org/10.1016/j.firesaf.2024.104141>

Received 10 November 2023; Received in revised form 18 February 2024; Accepted 27 March 2024

Available online 29 March 2024

0379-7112/© 2024 The Authors. Published by Elsevier Ltd. This is an open access article under the CC BY license (<http://creativecommons.org/licenses/by/4.0/>).

conducted to investigate the performance of FFFSs, e.g., the 1:23 scale tests by Ingason [18], the 1:10 scale tests with automatic sprinklers by Li and Ingason [19], the intermediate-scale tunnel tests by Blanchard et al. [20], the 1:4 scale water spray tests on design fires [21], the 1:4 scale tests on toxic gas production [22] and the 1:3 scale automatic sprinkler tests [23]. The focus of the literature review is on the suppression of fire development using water-based FFFSs in tunnels. Experiments with gas burners and numerical work are therefore not included. From these tests, it is recognized that FFFS can limit the fire growth and fire size, and prevent the fire spread to adjacent vehicles, thus reducing the required tunnel ventilation requirements. It also protects the tunnel structure, and reduces the need for passive structural protection, thus making significant construction and operational savings.

Depending on system operating pressure and water droplet size, FFFSs are usually divided into low pressure and high pressure FFFSs [1], while there are also low pressure water mist systems used in tunnels.

For the sake of simplicity and to be more precise, in this study, FFFSs are classified into three types: low pressure FFFS, medium pressure FFFS and high pressure FFFS. Below the characteristics of the individual systems are briefly described in combination with the large-scale tests mentioned above.

1.1. Characteristics of various FFFSs

All values on pressure and water density given in this section refer to full scale. A low pressure FFFS refers to a normal water spray system. Low pressure FFFSs in buildings and warehouses have been used for over 100 years. In buildings the systems are referred to as sprinklers as they usually use sprinklers with individual thermal activation mechanism whereas in tunnels open nozzles are activated in zones by an external operator, hence the use of the different acronym (FFFS) for tunnels. For ordinary and extra hazard occupancies, sprinklers are designed in accordance with NFPA 13 [24] or other recognized standards. The water density ranges from 6 mm/min to 16 mm/min, and the operating pressure ranges from 0.5 bar to 5.2 bar. Japan introduced low pressure FFFS into its high-risk urban tunnels in 1963 and a water density of 6 mm/min is typically used. Australia has installed low pressure FFFSs in road tunnels since 1992 [1] and the water density used is in the range of 7.5–10 mm/min. Sweden has installed its own large droplet low pressure FFFS in several tunnels such as the Stockholm Northern Link tunnels and the Götatunnel in Gothenburg, and the system is presently being installed in the new Stockholm Bypass tunnel system [2]. The typical water density used in Sweden is 10 mm/min. In the large-scale tests with low pressure FFFSs mentioned above, the water densities tested are in a range of 8–12.5 mm/min. The average water application rate for low pressure systems is around 10 mm/min, and the typical nozzle spacing for deluge systems is 3 m–5 m. The spray angle of the nozzles is typically between 120° and 160°. In most of those tests, effective fire suppression was observed, i.e., after activation of FFFS the fire development has been effectively reduced and the heat release rate (HRR) has been significantly lower than the maximum value obtained in a corresponding free-burn test. In this study, the default low pressure system refers to a water density of 10 mm/min.

High pressure FFFSs started to be used in the 1990s [4]. Referring to the definitions in NFPA 750 [25], high pressure water mist systems refer to operating pressures of 34.5 bar or greater. In the past two decades, the interest to use high pressure FFFSs has dramatically increased in Europe. In the large-scale tests with high pressure FFFSs mentioned above, the systems usually have an operating pressure between 35 bar and 80 bar and a water density between 2 mm/min and 5 mm/min. The typical coverage area for each nozzle is around 3.5 m × 3.5 m. The spray angle of the nozzles is mostly between 120° and 160°. In this study, the default high pressure system refers to a water density of 3.7 mm/min.

The medium pressure system is developed aiming to take advantage of both low pressure (effective fire suppression) and high pressure systems (effective gas cooling). The definition of a medium pressure FFFS is

not as clear as that of low pressure or high pressure FFFS. However, it is reasonable to assume that the water density and the operating pressure used lie between the low pressure system and the high pressure system. In this study, the water density for the default medium pressure system refers to 6.85 mm/min, i.e., the mean value of the water densities for the default low and high pressure systems. The operating pressure is in a range of 5.2–35 bar. Note that the medium pressure system defined here may refer to both the low pressure (12 bar or less) and intermediate pressure water mist systems (12–35 bar) as per NFPA 750 [25].

1.2. System configuration and activation mode

FFFSs in tunnels are mostly divided into individual zones, each of which covers a tunnel length of 20–50 m. In case of fire, two or three zones nearby the fire source will be activated, the so-called “deluge mode” [1]. There has also been interest to use automatic water spray systems in tunnels. No zones are needed but the so-called “sprinkler mode” [1] is applied, i.e., the sprinklers are automatically activated in case of fire and hot smoke, usually with the aid of the embedded bulbs or other heat sensitive elements. It has been found that they are suitable for tunnels with low ventilation velocities, but not for tunnels with high ventilation flows to avoid system failure, i.e., too many sprinklers are activated [19,23]. The studies in Refs. [17,21] also show that fully automatic sprinklers systems in tunnels are plausible for large fires and the activation temperature is important as well as water density. In this study, the deluge mode is used.

Most of the FFFSs have similar configurations in piping and nozzle placements in tunnels. Each nozzle covers a floor area of 8–16 m², and the spacing between nozzles is mostly between 3 m and 4 m. In this study, an average coverage area of 12 m² is assumed.

1.3. Research question

Despite many installations and tests, there is lack of general knowledge about how to design and optimize FFFS in tunnels with regard to pressure, water density and activation. The previous large-scale fire tests mostly focus on validating the performance of a specific system to be used in a given tunnel. No systematic study of the effects of different parameters has been conducted in the referred full scale tests. FFFS affects fire development by different suppression mechanisms, i.e., fuel surface cooling, gas cooling, dilution, radiation attenuation and kinetic effects [1]. High pressure FFFS is efficient in suppressing compartment fires. However, Heskestad [26] concluded that it is much more difficult to suppress fires with high pressure FFFS in spaces where appreciable oxygen depletion cannot take place. This conclusion is supported by tests by Arvidson [27]. The key mechanisms for low and high pressure FFFSs in tunnels and how they affect system performance have not been clearly understood.

One key question that needs to be answered is: which type of system performs most efficiently in suppression or control of different types of tunnel fires. To answer this question, various FFFSs were tested in a medium scale tunnel to investigate the fire suppression performance in different types of fire scenarios. In this study, the focus is on how efficient these different systems are in reducing the HRR and the energy released, and preventing the fire spread to nearby vehicles. Effects on gas temperatures and gas concentrations will be presented in separate publications.

2. Container tunnel fire tests

Carrying out a parametric study of numerous variables in a full scale tunnel is expensive and cumbersome. Small scale testing has also some limitations considering the scaling of water sprays and evaluation of system performance. The use of an intermediate size tunnel constructed using regular shipping containers was considered the best option available for this study. The Froude scaling was applied in the fire tests

performed. The scale ratio used in this study was 1:3. A summary of the scaling laws applied in the tests is given in Table 1. Details about the Froude scaling can be found in the literature [1]. The length scaling ratio was 1:3 (1 length unit in model scale tunnel corresponds to 3 length units in full scale tunnel) which results in the following: time, velocity and water density are square root of the length scale (1.73 times), water operating pressure is the length scale (3 times), and HRR is 5/2 power of the length scale (15.6 times). Gas temperature and gas concentrations are approximately the same in both scales.

2.1. Test tunnel

The container tunnel consisting of four standard shipping containers was 49.2 m long, 2.39 m high and 2.35 m wide, as shown in Fig. 1. The tunnel ceiling and the upper parts of the tunnel walls (a height of 0.6 m) were protected with 10 mm thick Promatect H boards, within the range of -2 m and $+4$ m. Within the range of -1.5 m and 1.5 m, the floor was also protected with Promatect H boards to avoid damage to the plywood floor. Outside the protected area, the walls and ceiling of the standard containers were made of corrugated steel sheets.

2.2. Ventilation

Two electric fans with a diameter of 0.71 m were placed outside of the tunnel inlet to create a longitudinal air flow in the tunnel. The fans were placed at 0.32 m and 1.35 m above the tunnel floor, close to the centre of the tunnel cross section, see Fig. 1. A frequency regulator was adjusted to obtain the design values within 0.6 m/s – 2.1 m/s used in most of the tests. Two perforated steel nets (70 % opening area) were used to regulate the flow. In most of the tests, a velocity of 1.8 m/s was applied but to further investigate the ventilation effects, a velocity of 1.2 m/s was also used in some scenarios. The corresponding full scale velocities are 3.1 m/s and 2.1 m/s, respectively.

2.3. Fire source

The goods carried by heavy goods vehicles (HGVs) may vary significantly. It is difficult to know which types of fuels will burn in an incident. Different types of fire sources were tested, including idle wood pallets, wood cribs, a mixture of wood and plastic cribs, and heptane pools. The fire sources were placed at around 26.6 m from the left tunnel portal, close to the longitudinal midpoint of the tunnel. The wood pallet fires refer to the situation where goods are densely packed with a small porosity, while the crib fires refer to the situation where goods are loosely packed with a large porosity.

Table 1

A list of scaling correlations for the model tunnel [1].

Type of unit	Scaling	Equation number
Heat Release Rate \dot{Q} (kW)	$\dot{Q}_M/\dot{Q}_F = (l_M/l_F)^{5/2}$	(1)
Velocity u (m/s)	$u_M/u_F = (l_M/l_F)^{1/2}$	(2)
Time t (s)	$t_M/t_F = (l_M/l_F)^{1/2}$	(3)
Energy content E (kJ)	$E_M/E_F = (l_M/l_F)^3$	(4)
Fuel mass m (kg) ^a	$m_M/m_F = (l_M/l_F)^3$	(5)
Temperature T (K)	$T_M/T_F = 1$	(6)
Gas concentration Y^a	$Y_M/Y_F = 1$	(7)
Air pressure P (Pa) ^b	$P_M/P_F = l_M/l_F$	(8)
Heat flux \dot{q} (kW/m ²) ^c	$\dot{q}_M/\dot{q}_F = (l_M/l_F)^{1/2}$	(14)
Water droplet size d (mm)	$d_M/d_F = (l_M/l_F)^{1/2}$	(15)
Water density \dot{q}_w (mm/min)	$\dot{q}_{w,M}/\dot{q}_{w,F} = (l_M/l_F)^{1/2}$	(16)
Water flow rate \dot{q}_w (l/min)	$\dot{q}_{w,M}/\dot{q}_{w,F} = (l_M/l_F)^{5/2}$	(17)
Water pressure P_w (bar) ^d	$P_{w,M}/P_{w,F} = l_M/l_F$	(18)

^aAssume the ratio of heat of combustion $\Delta H_{c,M}/\Delta H_{c,F} = 1$. l is the length scale. Index M is related to the model scale and index F to full scale ($l_M = 1$ and $l_F = 3$ in this study).

In the tests with solid fuels (idle wood pallets and wood/plastic cribs), the fire sources were mostly placed on a steel platform and on one side of the tunnel cross section, as shown in Fig. 2, while in two tests, the fire source was placed along the centerline of the tunnel. The platform consisted of a 0.55 m high steel frame and two layers of 10 mm thick Promatect H boards on top of it. In these tests, 2 mm thick steel covers were used to simulate the HGVs. Side curtain HGVs with plates on tops are commonly used due to the convenience in loading. There are also many HGVs having tarpaulins on both sides and the tops. The front and back sides, however, are typically closed with plates. Therefore, in all the tests except the pool fire tests, the front and back covers were placed. In most of the tests, a top cover was also applied. Note that a completely closed HGV, e.g., a steel container, is considered to have a lower fire hazard, and thus not of key interest and not tested in this study. Two small liquid pans were used as the ignition source, each having dimensions of 100 mm (L) \times 250 mm (W) \times 30 mm (H). These two pans were placed just behind the front cover, at the level of the lowest pallet or crib on the upstream side (see Fig. 2). They were about 10 cm from the front cover. In the idle wood pallet fires, each pan was filled with 150 mL heptane. In the wood crib tests and wood and plastic crib tests, each pan was filled with 300 mL heptane as it was more difficult to ignite the wood crib. However, in one test 450 mL heptane was used.

In the pool fire tests, the pool was placed along the center line of the tunnel, and at the floor level.

2.3.1. Wood pallet fires

The scaling method developed for scaling time-resolved burning behaviors of wood pallet fires [28] was applied. In the tests, the full scale European wood pallets (pine) were scaled down but the scaling laws are slightly modified, in the same way as in the literature [23]. The number of pallets in one direction is slightly reduced, while the dimensions in that direction are raised accordingly to fulfil the scaling laws for geometry, HRR, fire growth rate and energy content presented in the literature [28]. In each of the idle wood pallet fire tests, 72 wood pallets were used, consisting of 12 vertical layers and 6 piles longitudinally, as shown in Fig. 3. The full scale fire load refers to 8 (L) \times 2 (W) \times 21 (H) = 420 wood pallets. The wood pallets are made of pine. The humidity of wood pallets was mostly between 10 % and 11 %.

2.3.2. Wood crib fires

In the tests, both wood cribs and wood/plastic cribs (mixture of wood and plastic) were used as fire sources. The bottoms of the cribs were kept at 40 mm above the platform to facilitate the placement of the ignition sources beneath. The humidity of wood pallets was mostly around 12 %.

One crib consisted of 56 square long sticks, each having dimensions of 2.7 m (L) \times 0.045 m (W) \times 0.045 m (H), as shown in Fig. 4. The spacing between two neighboring sticks was 0.09 m. The porosity was around 4.3 mm, indicating a weak influence of porosity on the burning rate [29]. According to a previous study by Li et al. [30], in well-ventilated tunnels, there exists an upper limit for the heat release rate in wood fires, which is around 195 kW/m². As the exposed surface area is known, the maximum HRR can be estimated to be 5.3 MW, corresponding to 83 MW in full scale.

A steel stack was designed and used to place the sticks, as shown in Fig. 5. The sticks were placed on the eight layers of horizontal frames at the locations specified in Fig. 4. Each horizontal frame had a diameter of around 10 mm.

2.3.3. Wood and plastic crib fires

The configuration of a wood and plastic crib was the same as that of a wood crib. One wood and plastic crib had around 86% wood (48 sticks) and 14% plastic sticks (8 sticks). This ratio is close to the previous model scale tests with various cross sections [30] and the Runehamar tunnel fire test 1 conducted in 2003 [31]. Note that the red marked squares in Fig. 4 (b) refer to the plastic sticks.

The plastic used was high-density polyethylene (HDPE) with a

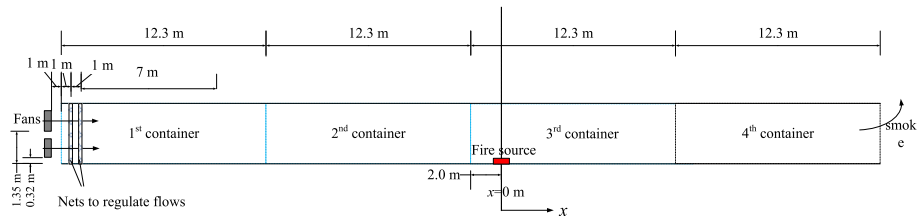


Fig. 1. A schematic drawing of the medium scale test tunnel (Side view).

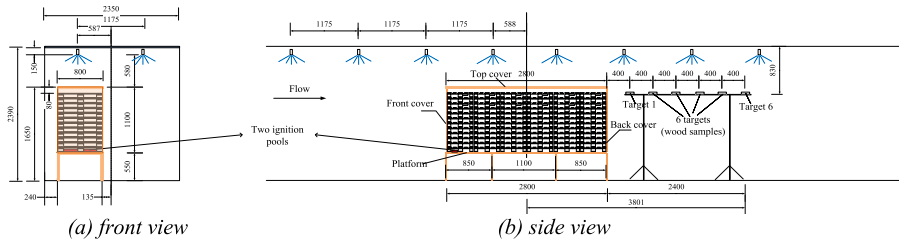


Fig. 2. Fuel arrangement for wood pallet fires in the tests. Dimensions are given in mm.

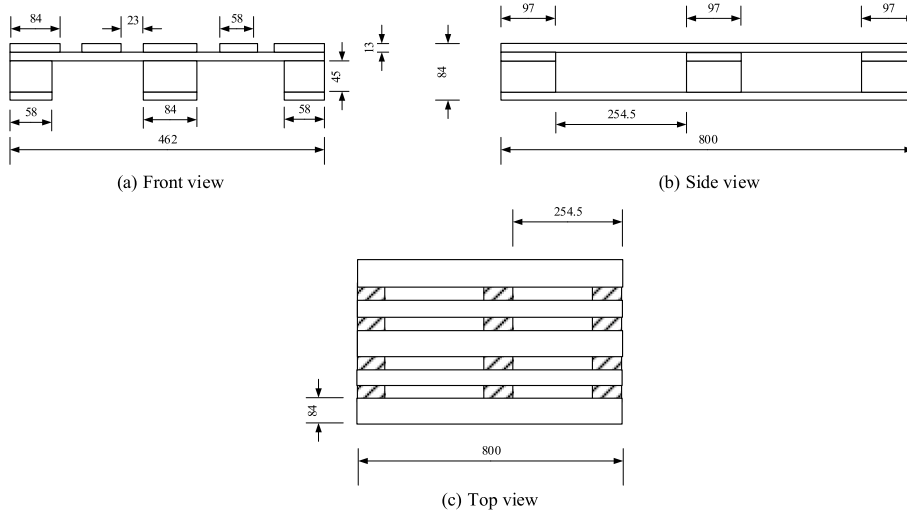


Fig. 3. Detailed drawing of the wood pallet [23]. Dimensions are given in mm.

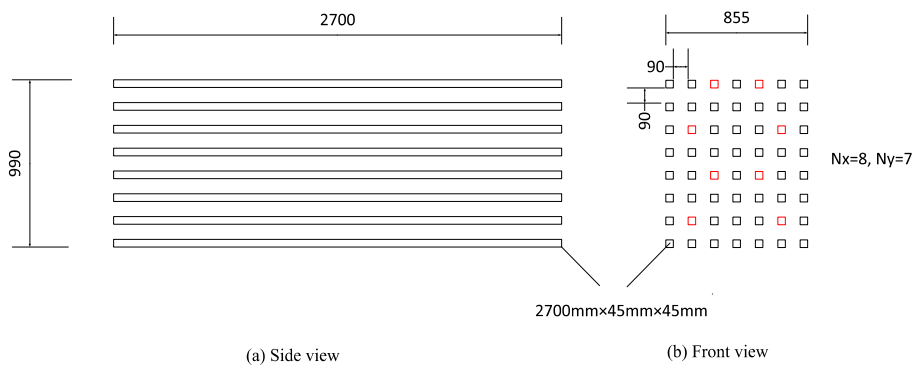


Fig. 4. Configuration of a crib. Dimensions are given in mm.

density of approximately 1000 kg/m^3 . The aim was to place the plastic sticks evenly within the crib, which usually was obtained but very cumbersome in labor. According to a previous study by Li et al. [30], in well-ventilated tunnels, the heat release rate per unit area for polyethylene is around 1000 kW/m^2 . Therefore, based on the exposed

surface area, the maximum HRR is estimated to be 8.4 MW, corresponding to 131 MW in full scale. This maximum HRR is in line with what was obtained in the Runehamar tests in 2003 [31].

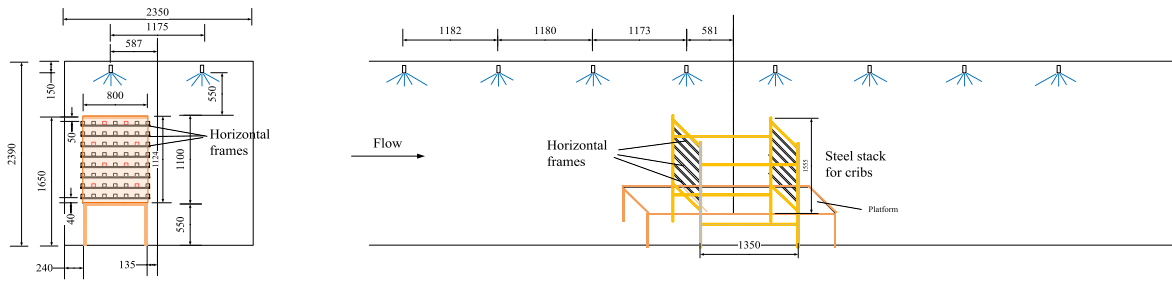


Fig. 5. Fuel arrangement for crib fires in the tests. Measures are given in mm.

2.3.4. Heptane pool fires

The dimensions of the pool were 0.5 m (L) × 0.8 m (W) × 0.12 m (H). Heptane was used as the fuel. In the tests with FFFS, 25 L of fuel were used, while 35 L was used in the free burn test.

2.4. Fire spread

In the tests with solid fuels, six wood samples were placed downstream of the main fire load at a height of around 1.6 m above floor, acting as “targets” to investigate the possibility of fire spread, as shown in Fig. 2. Each target had dimensions of 0.045 m (W) × 0.045 m (L) × 0.005 m (H). The target denoted “target 1” was closest to the fire source, 0.4 m from the downstream edge of the vehicle mock-up (end cover) or 1.8 m longitudinally from the fire source center. The furthest one was the one denoted “target 6”, positioned 3.8 m from the fire source center (corresponds to 11.4 m in full scale). The distance between the centers of two neighboring targets was 0.4 m. Notice that all the targets were placed within the water spray region.

2.5. Various FFFSs

Three types of FFFSs were tested (see Fig. 6). The nozzle used for the high pressure system was a multi-orifice nozzle, and the other two nozzles were single-orifice nozzles. Each system had two longitudinal rows of nozzles covering a spray region of around 9.4 m, corresponding to 28.2 m in full scale, as shown in Fig. 7. Each row consisted of 8 nozzles. The spacing between nozzles was 1.175 m, corresponding to 3.525 m in full scale. All nozzle outlets were positioned 0.15 m beneath the ceiling.

A summary of the nozzles tested for various FFFSs is given in Table 2. In this study, the default low, medium and high pressure FFFSs refer to water densities of 5.8 mm/min, 4 mm/min and 2.2 mm/min, respectively. The corresponding full scale values are 10 mm/min, 6.85 mm/min and 3.7 mm/min, respectively. For comparisons, in some tests, the water density of 4 mm/min was tested for both low pressure and medium pressure systems, and the water density of 2.9 mm/min was tested for both medium pressure and high pressure systems. The volume median diameters measured at 0.5 m below the nozzle are also given for information, but two data are predicted from the measured values at

other pressures for the same nozzle, with the aid of the correlation between operating pressure and droplet size: $d_m \sim p^{1/3}$ [1].

2.6. Instrumentation

A total of 125 measurement sensors were used, including 0.25 mm diameter thermocouples for gas and surface temperatures, plate thermometers for incident heat fluxes, bi-directional probes for velocities, gas analyses for gas concentrations and lasers for visibilities, as shown in Fig. 8. Between −18 m (upstream) and +5 m (downstream), ceiling thermocouples were placed every 0.59 m. The focus of the paper is on the HRR and the other measured variables will be presented separately.

The most important measurement in this study is the HRR, calculated by the oxygen consumption method with CO/CO₂ corrections based on the data measured 16.7 m downstream of the fire (Pile B). At Pile B, the gas temperatures and velocities were measured at 0.24 m, 0.6 m, 1.2 m, 1.67 m and 2.2 m above floor, and the gas concentrations were measured at 0.6 m, 1.2 m and 2.2 m above floor. While calculating the mass flow rate and heat release rate, the cross section at Pile B was divided into five segments in the calculations of the mass flow rate and heat release rate, following the methodology used for the previous Runehamar tunnel fire tests [32] and model scale fire suppression tests [22]. The velocity measurements are in the centre of each segment. A flow profile study was conducted close to the downstream tunnel portal using Testo 440 anemometer with closely evenly distributed 25 (5 × 5) measurement points across the cross section in order to validate and control the flow measurements. The longitudinal tunnel ventilation velocities (corresponding to ambient conditions), u_0 , were obtained based on the calculated mass flow rates. The heat release rates were estimated using the oxygen consumption method considering the production of CO and CO₂. The total HRR was the summation of HRR from these segments, determined by use of Eq. (1) [33]:

$$\dot{Q} = \sum_i \left[\Delta H_{O_2} \varphi_i - (\Delta H_{O_2, CO} - \Delta H_{O_2}) \frac{1 - \varphi_i}{2} \left(\frac{X_{CO,i}}{X_{O_2,i}} \right) \right] \frac{\dot{m}_i}{1 + \varphi_i(\alpha - 1)} \frac{M_{O_2}}{M_a} (1 - X_{O_2,i}) X_{O_2,i} \quad (1)$$

where the oxygen depletion factor, φ , is expressed as:

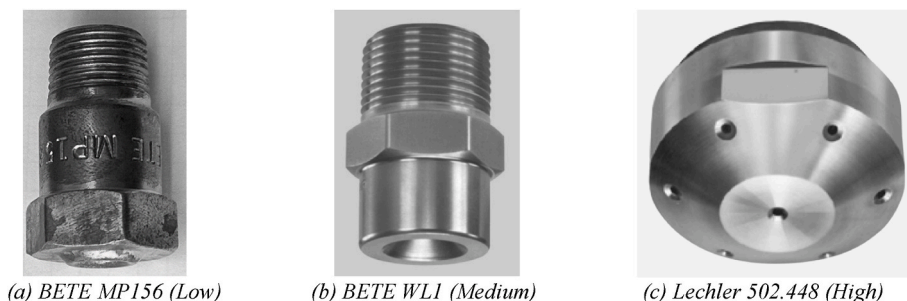


Fig. 6. Photos of the nozzles used in this study. Photo (a) was taken after the fire tests.

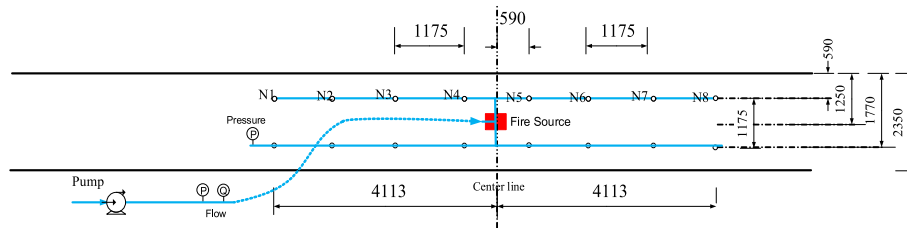


Fig. 7. A schematic drawing of the FFFS set up. Dimensions are given in mm.

Table 2
Summary of nozzles tested for various FFFSs.

FFFS System	Nozzle	Spray angle °	K-factor 1/(min·bar ^{1/2})	Narrowest hole diameter mm	Operating pressure, <i>p</i> bar	Water flow rate l/min	Water density		Volume median diameter, <i>d_m</i> µm
							model scale	full scale	
Low	BETE MP156	120	8.8	3.97	0.39	5.5	4.0	6.85	880
Medium	BETE WL1	120	2.35	2.08	0.82	8.0	5.8	10	861
					5.4	4.0	2.9	5.0	429 ^a
High	Lechler 502.448	~130	0.88	0.5	11.5	3.0	2.2	3.7	181
					20.5	4.0	2.9	5.0	149 ^a

^a This diameter was calculated based on the measured one for the same nozzle with the aid of the correlation: $d_m \sim p^{1/3}$ [1].

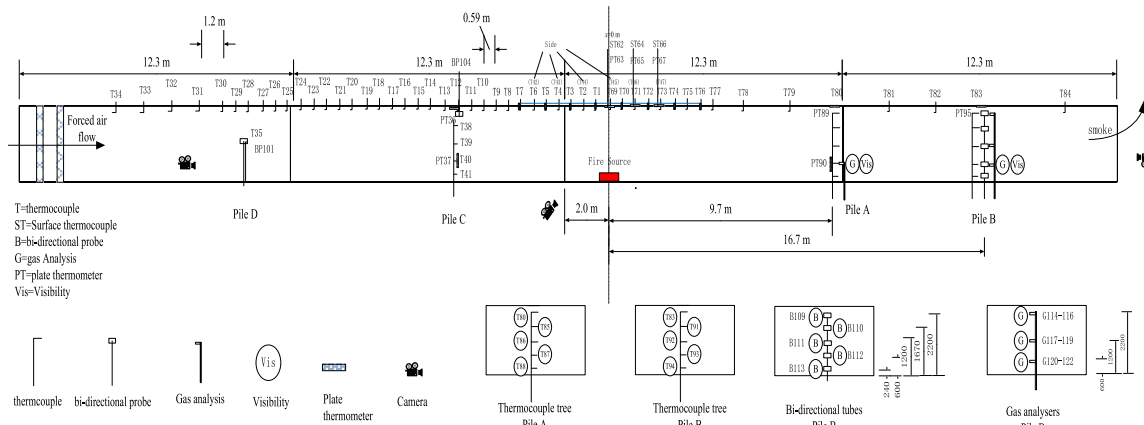


Fig. 8. Instrumentation and measurements (Side view).

$$\varphi = \frac{X_{0,O_2}(1 - X_{CO_2} - X_{CO}) - X_{O_2}(1 - X_{0,CO_2})}{(1 - X_{O_2} - X_{CO_2} - X_{CO})X_{0,O_2}}$$

and the mass flow rate of *i*th segment is:

$$\dot{m}_i = C_d \rho_i u_i A_i \quad (2)$$

The total mass flow rate is the sum of the mass flow rate of the five segments:

$$\dot{m} = C_d \sum_i \rho_i u_i A_i = \rho_0 u_0 A \quad (3)$$

In the above equation, \dot{Q} is the HRR (MW), ΔH_{O_2} is heat released per unit mass of O_2 consumed for complete combustion, $\Delta H_{O_2,CO}$ is heat released per unit mass of O_2 consumed for combustion of CO to CO_2 (17.6 MJ/kg), \dot{m} is the mass flow rate of the *i*th layer, *u* is velocity, u_0 is tunnel longitudinal velocity (tunnel average velocity at ambient conditions), C_d is the flow correction coefficient, *M* is molecular weight (kg/kmol), α is a constant (approx. 1.105), X_{0,O_2} is the volume fraction of oxygen in the incoming air (ambient), X_{0,CO_2} is the volume fraction of

carbon dioxide in the incoming air (ambient), and X_{O_2} and X_{CO_2} are the volume fractions of oxygen and carbon dioxide, respectively, as measured by a gas analyser (dry) at the measuring station downstream of the fire. The superscript 0 indicates the incoming fresh air flow and the superscript *i* indicates the *i*th segment. X_{0,H_2O} is the volume fraction of water vapor in the incoming fresh air flow prior to combustion (ambient). The upstream water spray may increase the water vapor concentration of the incoming flow but its influence on the HRR is considered small as the ambient temperature is low.

Note that due to the existence of boundary layers, the velocity measured close to the wall is usually lower than that measured in the centre of the tunnel cross section, although this effect is less for turbulent flows which is the case in this study. In the tests, five velocity measurement points were vertically distributed, so the boundary effect has been partially reflected in the velocity measurement close to the ceiling and the floor. However, the sidewall effects should still be considered. Another issue is related to the placements of the bi-directional tubes and other nearby accessories that are necessary for testing. For both reasons, a flow profile survey was conducted to determine the flow correction

coefficient C_d in Eqs. (2) and (3), which was found to be approximately 0.8. It is worth noting that this coefficient may be different for another tunnel or another measurement design, depending on the flow profile and the measurement installations. For a new experimental set up, flow calibration should always be done to improve the accuracy of velocity and HRR measurements. In this work, for further validation, this flow correction factor was used in HRR measurements (see Eq. (1)) against gas fires with known HRRs (ranging from 0.5 MW to 3 MW) and the good agreement further supports its use. The transportation time [1] from the fire location to Pile B was taken into account for all the flow parameters. The response time of the gas analyzers, i.e. mainly due to the transportation time from the measuring position inside the tunnel to the measuring cell inside the instrument, was also considered and found to be around 22 s.

At the measurement stations (Pile A and B), the water vapor was filtered before conducting gas analysis measurements, so its influence on the gas measurements was eliminated. However, the evaporated water vapor contained in the gas flow at the measurement station may affect the mass flow rate measurement. It is difficult to accurately assess its influence unless the water vapor concentration is well measured. Despite this, it is possible to roughly estimate it. The key parameter is the amount of water vapor that may be contained in the gas flow at the measurement station. The maximum possible value for the total amount of water vapor in the gas flow could be estimated using the lower value between the total water flow rate (assuming all water was evaporated) and the HRR divided by the heat of gasification of water (assuming all heat released was consumed to produce water vapor). The average value for the maximum water vapor volumetric concentration in these tests is estimated to be around 9.8%. However, the actual value is considered much smaller, due to three reasons: (1) only a portion of water was evaporated and much water went to drain; (2) only a portion of the heat released was consumed to produce water vapor and much heat was either lost to tunnel structure or left in the gas flow; and (3) a portion of water vapor may condense on the way to the measuring station due to the temperature decay along the tunnel. To sum up, in these tests, as the amount of evaporated water in the tunnel at the measurement station was considered to be much less than the total amount of the tunnel flow, uncertainty due to water vapor in the HRR estimation was deemed to be small. However, if the ventilation velocity is low, the water vapor concentration at the measurement points may be significant, and thus it may need to be measured and considered in the calculation of the heat release rate, see Refs. [33,34].

3. Test procedure

A total of 32 fire suppression tests was conducted, including 14 idle wood pallets fires (tests series 1), 10 wood crib fires (test series 2), 4 wood/plastic cribs (test series 3), and 4 pool fires (test series 4). Among these, four free burn tests (marked with bold text) were conducted without any FFFS to obtain reference data. A summary of these tests is given in Table 3, including some key results such as the fire spread results. The first number of a test no. refer to the test series, e.g., 201 refers to the test 01 in test series 2. In the first two columns, the free burn tests are marked in bold. The correlations between the water density and operating pressure can be found in Table 2. The longitudinal air velocity in the tunnel was mostly set as 1.8 m/s but it was 1.2 m/s in some tests. The values are only nominal ones as they may vary within a range of ± 0.1 m/s.

During the tests with solid fuels, the FFFSs were activated mostly when the maximum gas temperature measured beneath the ceiling reached a value of 141 °C as a detection criterion, in accordance with the previous large scale tests [3,35] and model scale tests [21,22]. In some wood crib fire tests, a higher fire detection temperature of 300 °C was applied. In test series 4 with pool fires, the ceiling gas temperature at the early stage was not so high, and a fixed activation time of 3.5 min was used, corresponding to a gas temperature of around 100 °C.

During each test, when no visible flame was observed from the portals and the observation window (where the side camera was), the measurement results were checked to confirm the fire extinguishment and the test was usually terminated after approx. 5 min.

4. Results and discussion

The following analysis focuses on comparing the performance of the default FFFSs in terms of reducing the HRR and the energy released, and preventing the fire spread, while the influences of various influencing factors on the system performance are also investigated. The HRRs from the four test series with different fire sources are presented in sequence. The free-burn test is presented and discussed at first, followed by the comparisons of the HRRs for various FFFSs without and with the top cover. Thereafter the influences of various factors, i.e., ventilation, water density and operating pressure and activation time, are analyzed. Note that in this study, the default low, medium and high pressure FFFSs refer to water densities of 5.8 mm/min, 4 mm/min and 2.2 mm/min, respectively. The corresponding full scale values are 10 mm/min, 6.8 mm/min and 3.7 mm/min, respectively. Furthermore, the tunnel air velocity defaults to 1.8 m/s unless otherwise stated in the following sections.

The maximum HRRs from the tests are given in Table 3. For each fuel type, the maximum HRR is obtained in the free burn test without FFFS, and it is 6.3 MW for the idle wood pallet fire, 4.5 MW for the wood crib fire, 7.5 MW for the wood and plastic fire, and 1.4 MW for the heptane pool fire. The proportion of energy that was released or consumed in each test, E/E_{tot} , is also given in Table 3 where E_{tot} refers to the total energy released in the corresponding free burn test. The energy released in a test is calculated from the integration of the HRR curve of the test. It can be seen that the energy release data generally follow the same trend as the HRR, i.e., a higher HRR usually corresponds to a higher proportion of energy released in the test.

In the presence of FFFSs, at the activation (141 °C), the HRR was within 0.3–0.4 MW (at approx. 4 min after ignition) in the wood pallet fire tests, while in the crib tests it was around 0.4 MW without top cover (approx. 2.8 min), and 0.5 MW (approx. 3 min) with the top cover. This corresponds to a heat release rate ranging from 4.7 (0.3) MW to 7.8 (0.5) MW in full scale. The corresponding activation times were mostly between 3 min and 5 min. The higher HRR at activation in the crib fire tests could be attributed to the loosely packed fuels where the fire plume can entrain more air before leaving the vehicle mock-up. In the crib tests, the presence of the top cover also increases the activation HRR, which should be related to the enhanced entrainment since in the case of the top cover two fire plumes towards both sides are formed. This effect, however, is not so significant in the idle wood pallet tests where the fuels are densely packed. In the wood crib tests with an activation temperature of 300 °C, the HRR at activation was about 0.8 MW (approx. 3.3 min), greater than that for the tests with an activation temperature of 141 °C, as can be expected. In the pool fire tests, the activation time was 3.5 min and the HRR was around 0.75 MW. The corresponding full scale values are around 12 MW, which is higher than what was stated earlier. Comparing these values with the maximum HRRs given in Table 3 shows that the maximum HRRs are usually much higher than the activation HRRs, indicating that the fire continues to develop to some extent after the system activation. However, it can be noted that for the wood crib fires without the top cover and the pool fires, the maximum HRRs are close to the activation HRRs, indicating that efficient and prompt fire suppression takes place after the system activation.

A summary of results related to the occurrence of fire spread based on visual observations of the wood samples (targets 1 to 6) after the fire tests is given in Table 3. “No” indicates that the target was not affected by the fire. “Burnt” indicates that the target was completely burnt, however, if only part of the target was burnt, the approximate percentage of the burnt part based on visual observations is given behind. “Charred” indicates that the target was only charred but not burnt. Note

Table 3
Summary of test series 1–4 on fire suppression.

Test no.	FFFS system	Fire source	Top cover	Nominal velocity	Water density	$T_{\text{detection}}$	\dot{Q}_{max}	E/E_{tot}	Fire spread to different targets (samples)					
				m/s	mm/min	°C	MW		1 (nearby fire)	2	3	4	5	6 (furthest)
101	Low	Wood pallets	Yes	1.8	4.0	141	3.4	68%	Charred	No	No	No	No	No
102	Low	Wood pallets	Yes	1.8	5.8	141	2.6	68%	No	No	No	No	No	No
103	Low	Wood pallets	No	1.8	5.8	141	0.8	16%	No	No	No	No	No	No
104 ^a	Low	Wood pallets	Yes	1.8	5.8	141	2.9	69%	No	No	No	No	No	No
105	Low	Wood pallets	Yes	1.2	5.8	141	2.4	54%	No	No	No	No	No	No
106	High	Wood pallets	Yes	1.8	2.9	141	3.1	73%	Burnt~80%	Charred	No	No	No	No
107	High	Wood pallets	No	1.8	2.2	141	3.7	81%	Burnt~10%	No	No	No	No	No
108	High	Wood pallets	Yes	1.8	2.2	141	2.7	60%	Burnt~10%	No	No	No	No	No
110	High	Wood pallets	Yes	1.2	2.2	141	3.1	74%	Burnt~80%	Burnt~60%	Charred	Charred	Charred	No
111	Medium	Wood pallets	Yes	1.8	2.9	141	2.7	71%	Charred	No	No	No	No	No
112	Medium	Wood pallets	Yes	1.8	4.0	141	2.7	65%	Charred	No	No	No	No	No
113	Medium	Wood pallets	No	1.8	4.0	141	1.4	36%	No	No	No	No	No	No
115	Medium	Wood pallets	Yes	1.2	4.0	141	1.8	38%	No	No	No	No	No	No
116	Free burn	Wood pallets	Yes	1.8	0	–	6.3	100%	Burnt	Burnt	Burnt	Burnt	Burnt	Burnt
200 ^a	Low	Wood crib	Yes	1.8	5.8	141	0.8	21%	No	No	No	No	No	No
201	Low	Wood crib	Yes	1.8	5.8	141	0.9	7%	No	No	No	No	No	No
202	Low	Wood crib	No	1.8	5.8	141	0.5	3%	No	No	No	No	No	No
203	Low	Wood crib	Yes	1.8	5.8	300	1.1 ^c	11% ^c	No	No	No	No	No	No
204	High	Wood crib	Yes	1.8	2.2	141	2.8	79%	No	No	No	No	No	No
205	High	Wood crib	No	1.8	2.2	141	0.6	3%	No	No	No	No	No	No
206 ^b	High	Wood crib	Yes	1.8	2.2	300	4.0	98%	Charred	No	No	No	No	No
207	Medium	Wood crib	Yes	1.8	4.0	141	1.0	38%	No	No	No	No	No	No
208	Medium	Wood crib	No	1.8	4.0	141	0.6	2%	No	No	No	No	No	No
210	Free burn	Wood crib	Yes	1.8	0.0	–	4.5	100%	Burnt	Burnt	Burnt	Burnt	Burnt	Burnt
301	Low	Wood and HDPE	Yes	1.8	5.8	141	2.4	55%	No	No	No	No	No	No
302	High	Wood and HDPE	Yes	1.8	2.2	141	5.9	68%	Burnt~70%	Burnt~40%	Burnt~30%	Charred	Charred	Charred
303	Medium	Wood and HDPE	Yes	1.8	4.0	141	4.9	61%	No	No	No	No	No	No
304	Free burn	Wood and HDPE	Yes	1.8	0.0	–	7.5	100%	Burnt	Burnt	Burnt	Burnt	Burnt	Burnt
401	Low	Pool fire	No	1.8	5.8	FT ^d	0.8(1.1 ^e)	~100%	NA					
402	High	Pool fire	No	1.8	2.2	FT ^d	0.8	~100%						
403	Medium	Pool fire	No	1.8	4.0	FT ^d	0.9	~100%						
404	Free burn	Pool fire	No	1.8	0	–	1.4	100%						

^a Centered fire source.

^b Centered fire source and 1.5 times the amount of ignition fuel.

^c Estimated based on test 201.

^d FT: Fixed Time.

^e During the period of malfunction, HRR increases to 1.1 MW.

that in the pool fire tests, the fire spread was not tested due to the different placement of the fire source. It is clearly shown that in the free burn tests with solid fuels, all the targets were burnt. In comparison, in the presence of the FFFS, the targets were usually not burnt. In these tests, the low pressure system performed well in terms of preventing fire spread, and only in test 101 with the lower water density of 4 mm/min the first target was charred. The medium pressure system also performed relatively well in preventing fire spread, and only in two tests the first target was charred. By contrast, the high pressure system performed less effective in preventing the fire spread. In the majority of the tests with the high pressure system (5 out of 8 tests), one or more targets were partially burnt. In the following sections, more detailed comparisons of fire spread will be made together with the HRR and the proportion of energy released.

4.1. Wood pallet fires

4.1.1. Free-burn test

The HRR curve from the free burn wood pallet fire test at a longitudinal velocity of 1.8 m/s with the top cover is shown in Fig. 9 (the black line). The fire develops steadily up until 16.5 min (when the HRR reaches around 4 MW). At 17.5 min, the HRR reaches 5 MW (78 MW in full scale), and after 0.1 min (17.6 min) the HRR suddenly rises to its peak of 6.3 MW (98 MW in full scale). This should be related to the collapse of the first wood pile on the upstream side, towards the side wall nearby, as observed in the test, which leads to a sudden increase in the total exposed fuel surface area and thus an immediate increase in the HRR. This phenomenon was also noticed in the previous tests [23,28]. In general, the peak HRR correlates well with the previous free burn test in 1:4 scale where the obtained peak HRR corresponds to 96 MW in full scale [21]. It is worth mentioning that in the 1:4 scale tests, besides the 50 pallets as the main fire load, 10 pallets were used as the target to evaluate possible fire spread and they were also involved in burning in that free burn test. However, in the current study, no wood pile was used as the target and therefore the fire load was slightly lower than that in the 1:4 scale tests.

4.1.2. Comparison of default FFFSs without top cover

The performances of the three default FFFSs in the idle wood pallet fires without the top cover are compared in Fig. 9. The activation HRR is within 0.3–0.4 MW (approx. 4 min). It is shown in Fig. 9 that the fire is effectively suppressed by the low-pressure system. After the activation

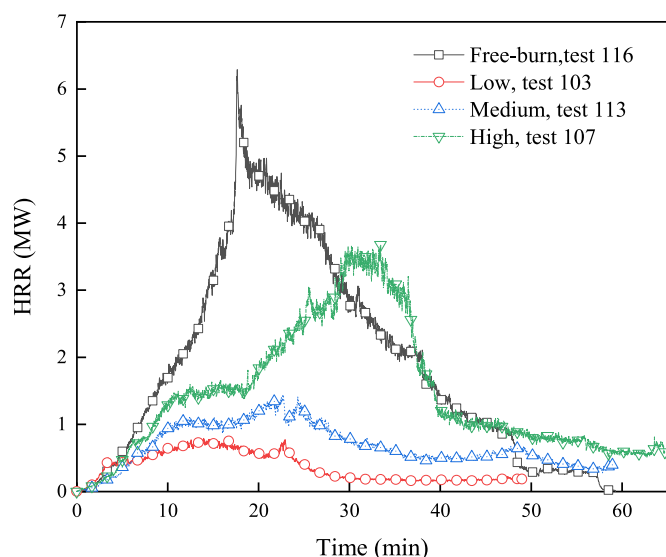


Fig. 9. HRRs in wood pallet tests with various FFFSs and without top cover ($u_0 = 1.8$ m/s). Data from the free-burn test is plotted for comparison.

of the low pressure system, the HRR increases slightly to its peak of 0.8 MW at 14 min, and the fire is almost extinguished after 25 min. By contrast, after the high pressure system is activated, the fire continues to increase until it reaches its peak of 3.7 MW at 33 min. For the medium pressure system, the peak HRR of 1.4 MW is reached at 23 min. Clearly, in terms of reducing the HRR, the low pressure system performs best, the medium pressure system performs moderately well, and the high pressure system performs worst. The influence on the gas temperatures shows a similar trend and it will be presented in a separate paper.

The results indicate that the system performance, in terms of efficiency in reducing the HRR, is improved as the water flow rate increases and the operating pressure decreases. This should be attributed to three factors. Firstly, larger droplets from a lower pressure nozzle can better penetrate the fire plume. Secondly, a higher water flow rate cools down the fuel surfaces more effectively. Thirdly, the influence of forced air flow on the trajectories of larger droplets is less in comparison to very fine droplets which may be carried away by the air flow for a long distance before hitting the fire load or tunnel floor, as shown by Rein et al. [36].

From Table 3, the same trend can be found for the proportion of energy released in the tests (16%, 36% and 81% for the low, medium and high pressure systems, respectively). Furthermore, there was no fire spread to the targets in the tests with the low and medium pressure systems, however, the first target was partially burnt in the test with the high pressure system. It should be noted that the fire spread is affected not only by the amount of water delivered to the targets, but also by the heat exposed to the targets, which depends on the HRR, the ventilation velocity, and the gas cooling and radiation attenuation effects of the water droplets. The results of fire spread should be considered as the combined effect of these two factors.

4.1.3. Comparison of default FFFSs with top cover

The performances of the three default FFFSs in the idle wood pallet fires with the top cover at 1.8 m/s are compared in Fig. 10. The activation HRR is within 0.3–0.4 MW at approx. 4 min. The maximum HRRs for the default low, medium and high pressure systems are 2.6 MW, 2.7 MW and 2.7 MW, respectively. They are rather close to each other, and only show an insignificant decrease of HRR with the increasing water density. The fire curves are also similar. The characteristics of the low pressure system resulted in improved results compared to others at the early stage (before 12 min), which could be related to the strong

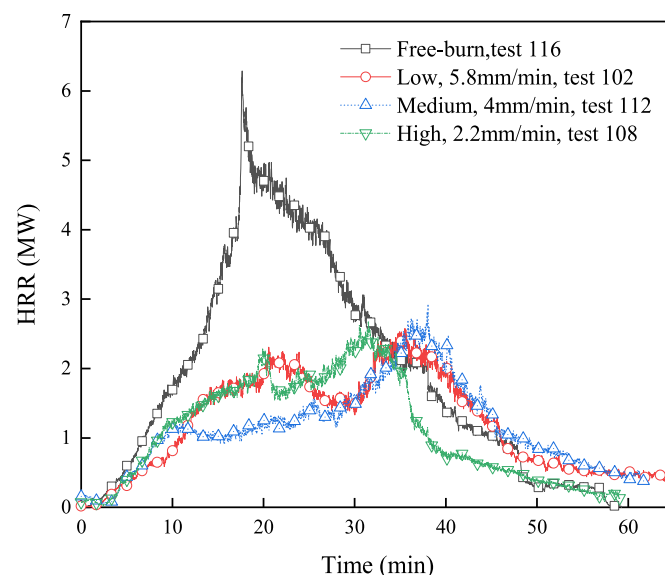


Fig. 10. HRRs in fire suppression tests with top cover ($u_0 = 1.8$ m/s). Data from the free-burn test is plotted for comparison.

penetration capacity of the large droplets. However, between 12 min and 26 min, the medium pressure system performs better. After 26 min, the HRR curves for the low and medium pressure systems are close to each other. Between 12 min and 20 min, the HRRs for the low and high pressure systems are almost the same.

The results from these tests with the top cover as presented in Fig. 10 are very different to the results without the top cover presented in Fig. 9, which justifies the influence of the top cover. One may probably expect that with the top cover, fire suppression is much more difficult to achieve as the water cannot be directly discharged to a large portion of the fuels beneath the top cover. This appears to be true for the low and medium pressure systems. However, it is not the case for the high pressure system which performs slightly better with the top cover. After 20 min, the HRR without the top cover is higher, with a peak of 3.7 MW, compared to 2.7 MW with the top cover. This indicates that the key suppression mechanisms of the high pressure system differ from those for the low and medium pressure systems. The performance of the high pressure system relies more on gas cooling and dilution, thus requiring finer droplets, whereas the performance of the low pressure system relies more on fuel surface cooling, thus requiring a higher water density and larger droplets. The key suppression mechanism of the medium system appears to be more similar to the low pressure system. These results are very much in line with the large scale tests carried out by Arvidson [27] on cargo in a ferry setup in a fire laboratory (no longitudinal flow) using different top cover configurations, pressures and flow rates.

As shown in Table 3, the proportions of energy released in these tests are similar (68%, 65% and 60% for the low, medium and high pressure systems, respectively). However, there is a clear difference in the fire spread between these tests. There was no fire spread for the low pressure system. The first target was charred for the medium pressure system, and it was partially burnt for the high pressure system. This indicates that the risk of fire spread increases from the default low pressure system, the default medium pressure system to the default high pressure system. This seems to be intimately related to the water density and not so much to the radiation attenuation as one could anticipate.

For comparison, the results for the three default FFFSs at a longitudinal ventilation velocity of 1.2 m/s are plotted in Fig. 11. The activation HRR is about 0.3 MW at approx. 3.2 min. This value is slightly less than that at 1.8 m/s, as the temperature is inversely proportional to the velocity [37]. As no free burn test was performed at 1.2 m/s, the free-burn HRR curve at 1.8 m/s is plotted as a reference. At the lower velocity of

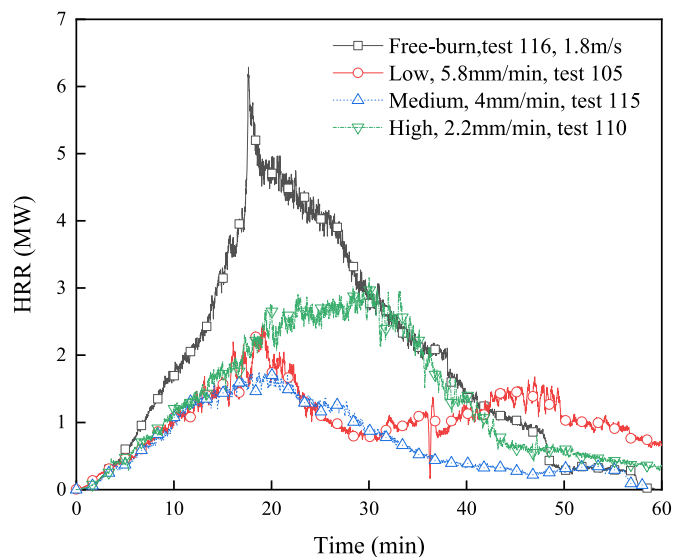


Fig. 11. HRRs in fire suppression tests with top cover ($u_0 = 1.2$ m/s). Data from the free-burn test (1.8 m/s) is plotted for comparison.

1.2 m/s, the default low and medium systems produce similar results for the first 30 min (except for a short period of around 20 min), but for the low pressure system, the fire redevelops after 30 min although the second peak HRR is lower. By contrast, the high pressure system performs considerably less effectively. The HRR continues to increase until it reaches its peak of 3.1 MW at 32 min. This also resulted in large portions of the first two targets (about 80% and 60%) being burnt and three more targets being charred in the test with the high pressure system, whereas there was no fire spread for the low and medium pressure systems, as shown in Table 3. The proportion of energy released in the test is 54%, 38% and 74% for the low, medium and high pressure systems, respectively. The higher proportion observed for the low pressure system as compared to the medium pressure system is mainly attributed to the redevelopment of the fire after 30 min.

4.1.4. Influence of ventilation velocity for individual default systems

The effects of the longitudinal ventilation velocity on the performance of individual default systems are shown in Fig. 12. For the low pressure system, the maximum HRRs at the two velocities (1.8 m/s and 1.2 m/s) are close to each other, but the lower velocity seems to have a positive effect on the system performance. At 1.2 m/s, the fire reaches the maximum HRR at around 19 min and starts to decay afterwards, and the corresponding time at 1.8 m/s is around 35 min. For the medium pressure system, the maximum HRR at 1.8 m/s is much higher. Similar to the low pressure system, the fire decays earlier at the lower velocity. From Table 3, less energy is released at the lower velocity for both the low and medium pressure systems, i.e., the proportion of energy released is 54% at 1.2 m/s compared to 68% at 1.8 m/s for the low pressure system, and 38% at 1.2 m/s compared to 65% at 1.8 m/s for the medium pressure system. To sum up, a decrease in velocity from 1.8 m/s to 1.2 m/s improves the performance of the low and medium pressure systems. This could be related to the slower fire growth at the lower velocity [1], thus allowing more time for the suppression systems to take effect.

By contrast, the results for both HRR and energy released are different for the high pressure system. The performance at 1.2 m/s is not as effective compared to that at 1.8 m/s. The maximum HRR at 1.2 m/s is 3.1 MW, compared to 2.7 MW at 1.8 m/s. As expected, more energy is released in the test with the lower velocity for the high pressure system. Specifically, the proportion of energy released is 74% at 1.2 m/s compared to 59% at 1.8 m/s, as shown in Table 3. Regarding fire spread, the results for the lower velocity are also worse, with more targets being burnt or charred at 1.2 m/s. One probable reason could be that a higher velocity increases the longitudinal travel distance of the fine droplets. This indicates that droplets from nozzles positioned further upstream of the fire can have a positive influence on the fire size, thereby increasing the effects of gas cooling and dilution, and possibly surface cooling.

4.1.5. Influence of water density for individual systems

Water density is a key parameter for a FFFS. The required water density in an engineering design is usually related to the fire load and its configuration. In this section, results from the tests with varying water densities are presented for individual systems. It should be noted that, for a given system, an increase of the water density also increases the operating pressure, thereby resulting in finer water droplets. Therefore, this section investigates the combined effects for individual systems.

Fig. 13 shows how different water densities affect the performances of the individual systems. For the low pressure system, increasing the water density from 4 mm/min to 5.8 mm/min reduces the maximum HRR from 3.4 MW to 2.6 MW, whereas the energy released in the tests is very similar, as shown in Table 3. In both tests, there was no fire spread to the targets. For the medium pressure system, the increase of water density from 2.9 mm/min to 4 mm/min delays the early fire development between 10 min and 30 min, although the maximum HRRs are both around 2.7 MW. The energy released in the test with 2.9 mm/min is slightly higher, as shown in Table 3. In both tests, the first target was

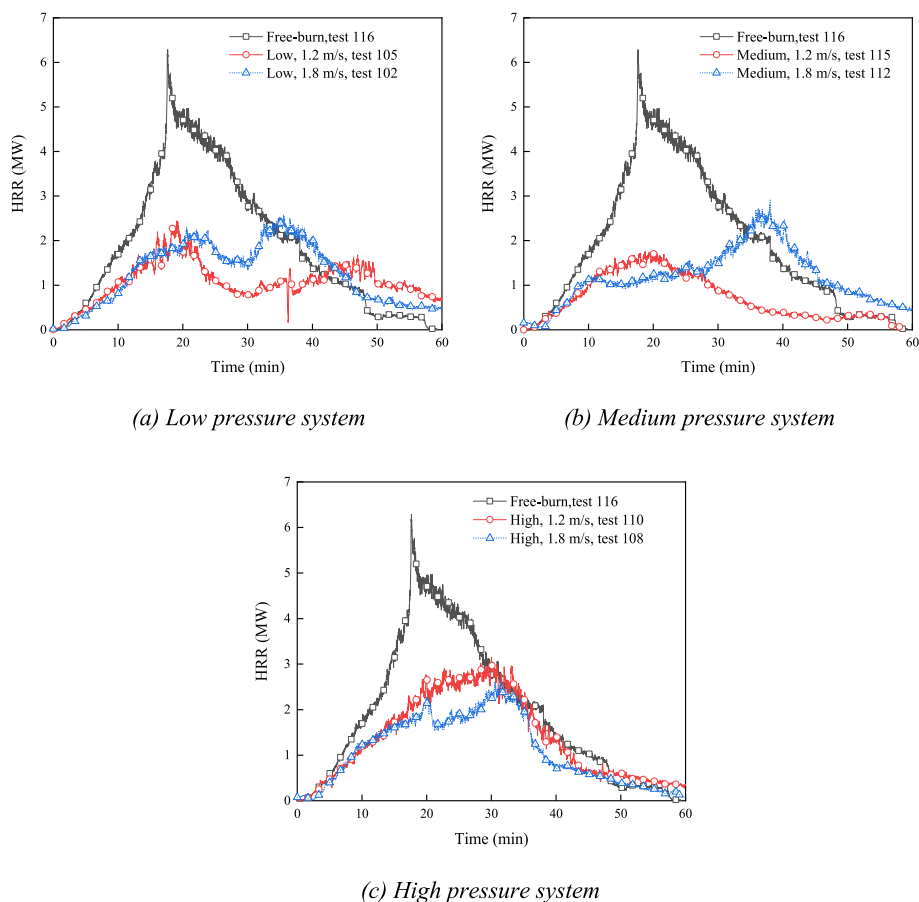


Fig. 12. Influence of the ventilation velocity on the system performance.

charred. For the low and medium systems, as expected, improved performance is found at higher water densities. This should be related to the improved ability to penetrate fire plumes and the greater cooling effect on fuel surfaces.

For the high pressure system, the increase of water density from 2.2 mm/min to 2.9 mm/min shows an insignificant influence on the fire suppression performance. As a matter of fact, it can be noticed that the high pressure system with the higher water density even performs slightly worse, i.e., both the maximum HRR and the energy released are slightly higher. Moreover, from Table 3, at 2.9 mm/min, the first target was burnt approximately 80 %, compared to 10% at 2.2 mm/min, and the second target was charred while it was not at 2.2 mm/min.

The slightly reduced performance at the higher water density could be related to the weaker penetration capability of finer droplets and the greater influence of ventilation on the trajectories of water droplets. Note that for a given system, a higher water density refers to a higher operating pressure, and thus finer droplets. The results indicate that the positive effect of the increased water density was counteracted by the negative effect of finer droplets for the high pressure system. In other words, too small water droplets are not as beneficial to the system performance for these wood pallet fires as with larger droplets. The main reason is the ability of larger droplets to penetrate through the fire plume down to the fuel surface where the water droplets cool the fuel surface.

4.1.6. Comparing different FFFSs with same density but different operating pressures

In the last section, the influence of water density on individual systems was investigated, however, the operating pressures were varied accordingly for a given system. Therefore, the combined effects of water density and operating pressure were investigated. As the main task of

this study is to find an optimal system, it is of interest to know how the operating pressure solely affects the system performance. Therefore, the results from different systems with same water densities are directly compared below.

Note that the low pressure test 101 and the medium pressure test 112 had the same water density of 4 mm/min, but different operating pressures. The influence of operating pressure on the fire suppression performance can thus be reflected in Fig. 14(a). The increase of the pressure appears to be beneficial to the fire suppression performance. The maximum HRRs are 3.4 MW for the low pressure system and 2.7 MW for the medium pressure system with the same water density of 4 mm/min. However, it should be noted that the corresponding nozzle operating pressure for the low pressure system is around 0.4 bar, which is close to its lower pressure limit. Table 3 shows that the energy released in these tests is very similar, and the first target was charred in both tests.

Furthermore, the results for the medium and high pressure systems with the same water density of 2.9 mm/min but different operating pressures (2.9 bar and 20.5 bar respectively) are compared in Fig. 14(b). The increase of the pressure from 2.9 bar to 20.5 bar reduces the system performance at the early stage (before 20 min). The medium pressure system with 2.9 bar slows down the initial fire development, although the results are quite similar after 20 min. This trend is different to the comparison of the low and medium pressure systems shown in Fig. 14(a). It can be seen from Table 3 that the energy released in these two tests is almost the same. However, the possibility of fire spread differs. In test 106 with the high pressure system at 20.5 bar, approximately 80 % of the first target was burnt and the second target was charred, whereas in test 111 with the medium pressure system at 2.9 bar, only the first target was charred.

This indicates that there may exist an optimal operating pressure that

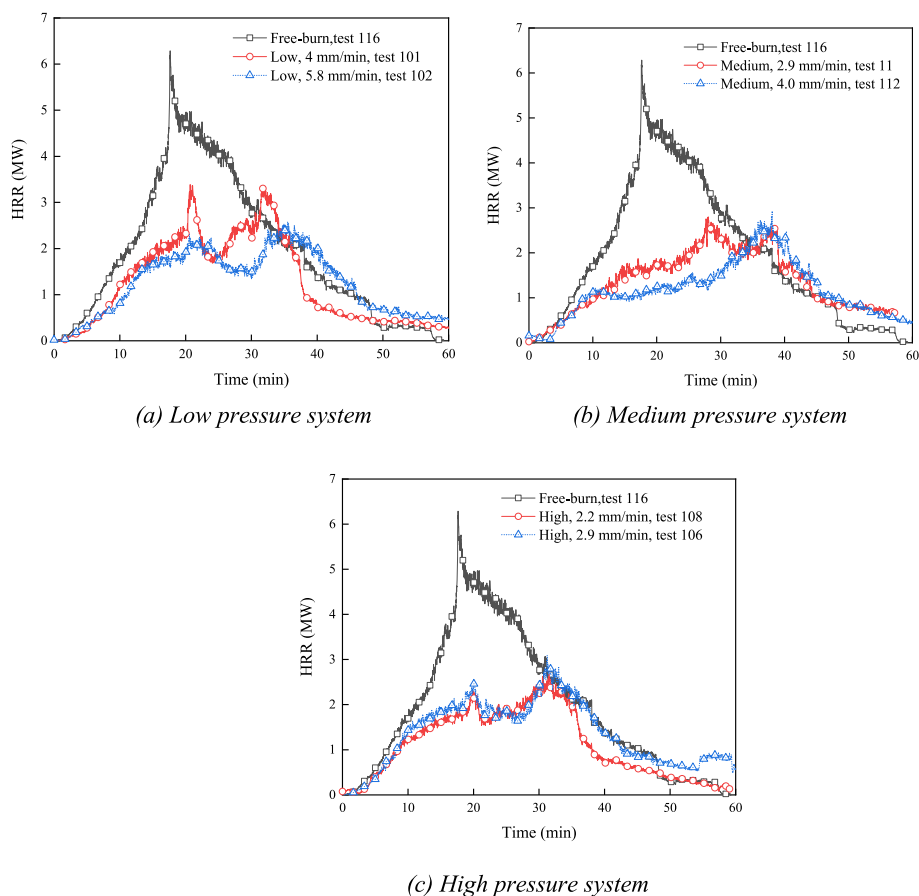


Fig. 13. Influence of water density on the system performance (1.8 m/s).

lies between the low pressure and the high pressure system. The physical explanation is that such a system takes advantage of both strong penetration of the droplets through the fire plume and efficient cooling during the transportation towards the fuel surface and when it hits the fuel surface. Due to the relatively larger difference between the performances of the low and medium pressure systems as shown in Fig. 14(a) compared to that between the medium and high pressure systems as shown in Fig. 14(b), it is probable that the optimal pressure lies between the operating pressures for the low and medium pressure systems. This, however, does not mean that the default medium pressure system generally performs better than the default low pressure system, as the conclusion here is made for a given water density. As is valid for all scale modelling, a confirmation of these results in a full scale tunnel would be beneficial, but this parametric study indicates how to design such full scale tests in a tunnel.

4.1.7. Side and centered wood pallet fires

In one idle wood pallet fire test (test 104), the fire source was placed at the centre line of the tunnel (centered fire source). The results are compared with those from the corresponding test with the default side placement (test 102) in Fig. 15. The HRRs are similar, but the fire development for the side placed fire source is slightly delayed. This may be due to the lower velocity on the side close to the wall, as it is known that the fire growth becomes slower at a lower velocity [1]. However, Table 3 shows that in both tests, the energy released is almost the same and the fire had no impact on the targets.

4.2. Wood crib fires

4.2.1. Free-burn test

The HRR curve from the free burn wood crib fire test at 1.8 m/s is

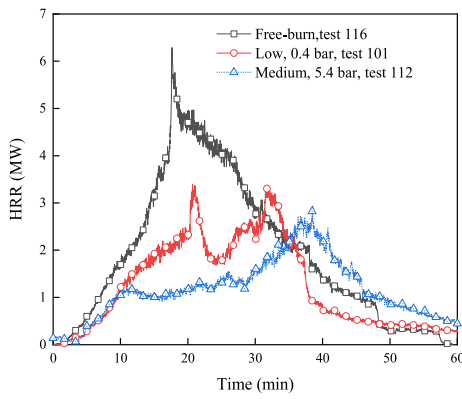
shown in Fig. 16 (the black line). The fire develops very rapidly after ignition and reaches the maximum HRR of 4.5 MW at 4.1 min, after which it starts to decay. Note that the maximum HRR is slightly lower than the estimate of 5.3 MW presented earlier. The reason could be that in the previous estimate, the upper limit for the heat release rate per unit area of 195 kW/m^2 was used. The results from this free burn test give a value of 165 kW/m^2 instead.

4.2.2. Comparison of default FFFSs without top cover

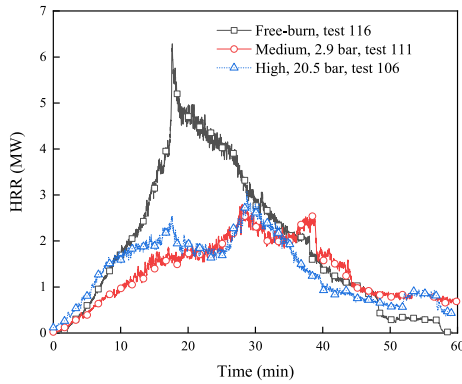
Fig. 16 shows the HRRs for the three default FFFSs in the wood crib fires without the top cover. The activation HRR is around 0.4 MW at approx. 2.8 min. All of the default systems perform very well. The differences are minor, although the maximum HRR slightly decreases with the increasing water density. In all of these tests, the fire HRR at the activation is around 0.4 MW. After activation, it takes around 15 s for the suppression systems to take full effect, and thereafter the fire decays rapidly. Clearly, the results are rather different to those for the densely packed wood pallet fires (Fig. 9). This indicates that an effective suppression can be more easily achieved for uncovered fires with loosely packed fuels. This should be related to the fact that it is much easier for water droplets to reach the inner side of the loosely packed fire load. As shown in Tables 3 and in these tests, the energy released is similar (2%–3%) and the fire had no impact on the targets.

4.2.3. Comparison of default FFFSs with top cover

The results from the wood crib fires with the top cover are shown in Fig. 17. The activation HRR is around 0.5 MW at approx. 3 min. The maximum HRRs for the default low, medium, and high pressure systems are 0.9 MW, 1 MW and 2.8 MW, respectively. Overall, the default low pressure system performs best, and the fire is completely extinguished after around 7 min. The fire with the medium pressure system is



(a) 4 mm/min density. Test 101 (0.4 bar) and Test 112 (5.4 bar).



(b) 2.9 mm/min. Test 111 (2.9 bar) and Test 106 (20.5 bar).

Fig. 14. Influence of operating pressure for different FFFSs with same density.

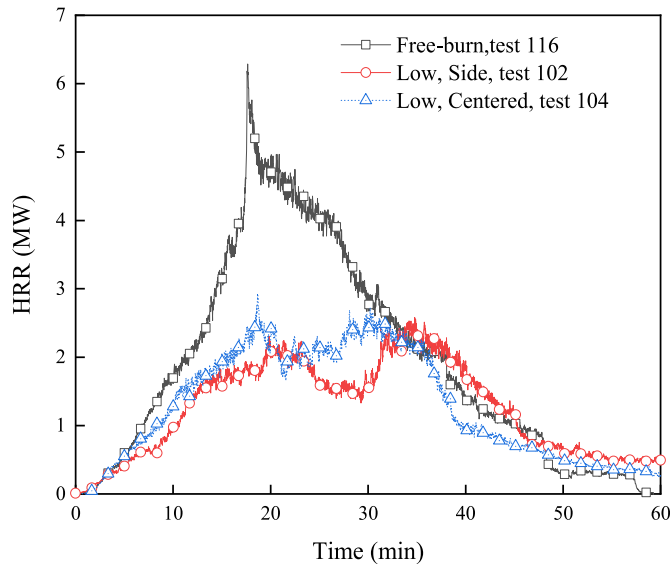


Fig. 15. Comparison of results of side and centered fires.

effectively suppressed but not extinguished after the system activation. It continues to burn for around 30 min at a relatively low level (less than 1 MW). For the high pressure system, the fire continues to burn intensely after the system activation, and reaches a maximum HRR of 2.8 MW at 7.6 min, significantly higher compared to the other systems. This is also reflected in Table 3, where the proportion of energy released is 7%, 38% and 79% for the low, medium and high pressure systems, respectively.

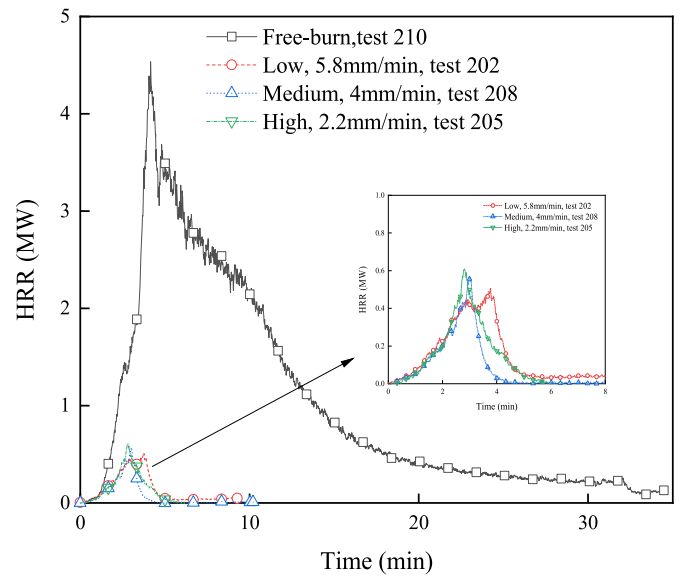


Fig. 16. Comparison of HRRs for various FFFSs in the wood crib fires without top cover.

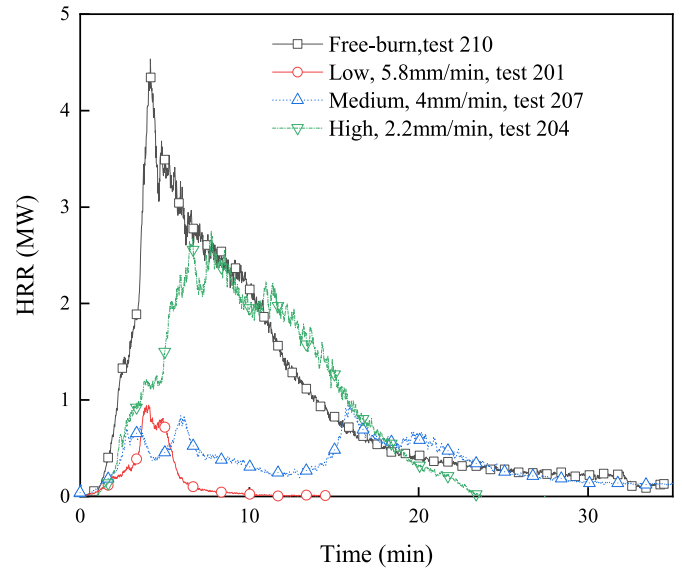


Fig. 17. Comparison of HRRs for various FFFSs in the wood crib fires with top cover.

Despite this, the fire had no impact on the targets.

The results shown in Fig. 17 are very different to those for the wood pallet fires with the top cover (Fig. 10) where the fires were not effectively suppressed using the default systems. This further confirms that an effective suppression can be more easily achieved for loosely packed fuels using the low pressure and medium pressure systems, as observed from the tests without the top cover. But this is not the case for the high pressure system, which does not effectively suppress the fire. This could be related to the weakened dilution effect due to the relatively better ventilation inside the loosely packed wood crib, compared to the densely packed wood pallets.

4.2.4. Side and centered wood crib fires for low pressure system

In test 200 with the low pressure system, the wood crib was placed along the centerline of the tunnel. The results are compared to test 201 where the fire source was placed on the side of the tunnel, as shown in Fig. 18. Both fires are effectively suppressed. The maximum HRRs are

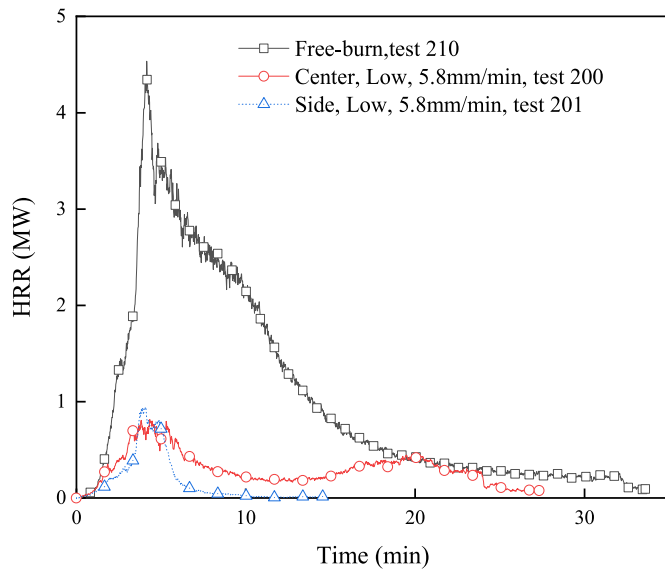


Fig. 18. Comparison of HRRs for centered and side wood cribs fires.

close to each other, while the duration of the centered fire is longer, thus resulting in a greater proportion of energy released in the test. Furthermore, in both tests, there was no fire spread to the targets, as shown in Table 3.

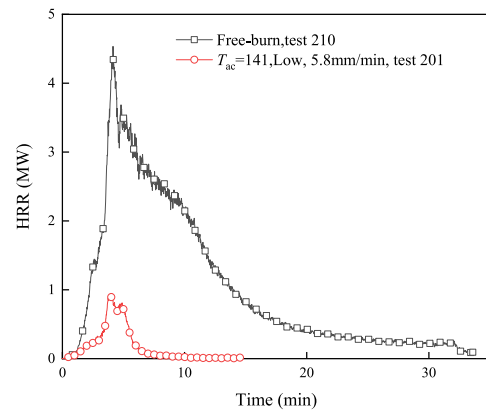
Overall, the different fire source locations (centered or side) have limited influences on the performances of the low pressure system, for both wood pallet fires and wood crib fires. In most of the tests, the fire source was placed on one side, as can be expected in most fire scenarios where the driver stops the incident vehicle on its lane.

4.2.5. Influence of activation criterion for low and high pressure systems

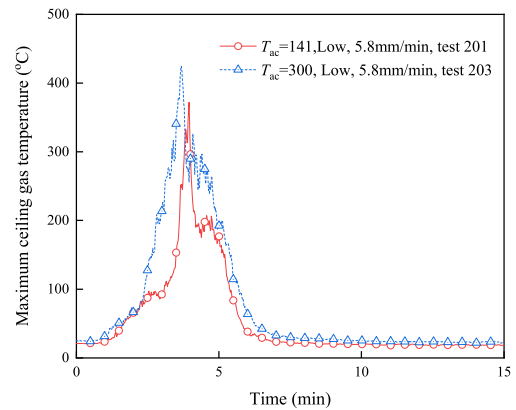
Different activation temperatures ($T_{ac} = 141\text{ }^{\circ}\text{C}$ or $300\text{ }^{\circ}\text{C}$) were used in some tests with the low and high pressure systems. In the tests with an activation temperature of $300\text{ }^{\circ}\text{C}$, the HRR at the activation is approximately 0.8 MW (approx. 3.3 min).

Unfortunately, in test 203 with the activation temperature of $300\text{ }^{\circ}\text{C}$, the gas analyzers malfunctioned. The HRR curve of test 201 is shown in Fig. 19(a), and the measured maximum gas temperatures beneath the tunnel ceiling from test 201 and test 203 are compared in Fig. 19(b). The temperatures were measured by thin thermocouples and radiation was not corrected but its effect was considered small due to the small size of the thermocouples. From Fig. 19(b) it can be observed that the measured gas temperatures decrease rapidly after activation and at around 7 min the temperatures are close to ambient. This indicates that both fires were effectively suppressed by the low pressure system for both activation temperatures and is partly confirmed by the HRR curve of test 201 shown in Fig. 19(a). It is known that without a FFFS or prior to its activation, the heat release rate is proportional to the ceiling excess gas temperature [37]. By analogy to the data of test 201, a rough estimation gives a maximum heat release rate of 1.1 MW for test 203, compared to 0.9 MW in test 201. From Table 3, the proportion of energy released in the tests is insignificant (7% in test 201 and 11% in test 203), and there was no fire spread to the targets in both tests. To sum up, the use of the higher activation temperature of $300\text{ }^{\circ}\text{C}$ has an insignificant effect on the performance of the low pressure system under the conditions tested. The default low pressure system is able to suppress the covered wood crib fires efficiently even with a late activation. This, however, may not be the case for the other systems.

The comparisons of the HRR curves for the high pressure system with the two different activation temperatures are shown in Fig. 20. It should be noted that in test 206 with the activation temperature of $300\text{ }^{\circ}\text{C}$, the fire source was placed at the center line of the tunnel, instead of the side



(a) HRR curves



(b) Measured maximum gas temperatures beneath tunnel ceiling

Fig. 19. Influence of activation temperature in wood crib fires with top cover for low pressure system.

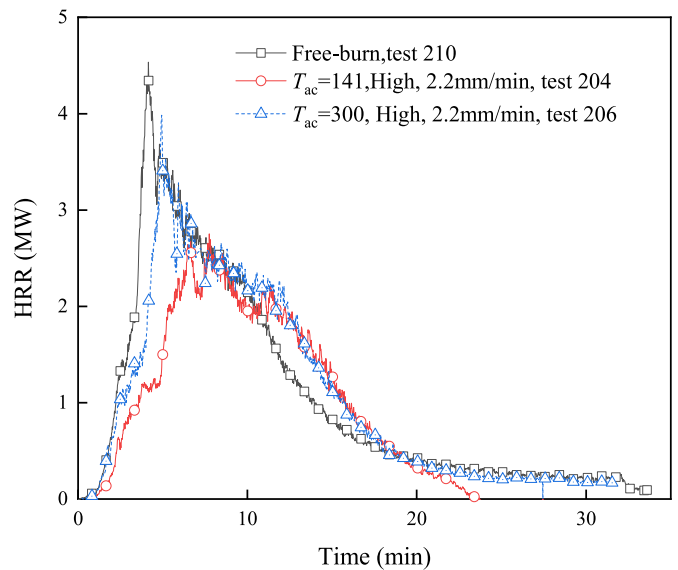


Fig. 20. Influence of activation time in wood crib fires with top cover for high pressure system.

by default as in test 204, and the amount of heptane used for ignition was 1.5 times the default amount. Therefore, they are not completely comparable. However, from the results for the low pressure system, it

was observed that the two different fire source location could have insignificant impacts on the fire suppression performance. Furthermore, the slight increase in the amount of ignition fuels in test 206 (1.5 times that of test 204) may only have an influence on the initial development and its effect is considered small after the system activation ($HRR = 0.8$ MW).

It can be seen in Fig. 20 that the HRR curve of test 206 with the activation temperature of $300\text{ }^{\circ}\text{C}$ is very close to the free-burn test. The maximum HRRs are 2.8 MW and 4 MW for activation temperatures of $141\text{ }^{\circ}\text{C}$ and $300\text{ }^{\circ}\text{C}$, respectively. This indicates that in case of a late activation for the high pressure system, the suppression becomes much more difficult, resulting in a higher maximum HRR. Moreover, the fire growth rate (the slope of the HRR curve) with the late activation is much steeper than that of test 204. One reason could be the slightly larger ignition source used in test 206. However, the ignition source burnt out at around 3 min ($HRR = 1$ MW), so its influence on the continued fire development involving FFFS is considered insignificant. As shown in Table 3, the proportion of energy released in these tests is significant (79% in test 204 and 98% in test 206). The first target was charred in test 206 with the activation temperature of $300\text{ }^{\circ}\text{C}$ but not in test 204.

Conclusively, delayed system activations usually result in higher maximum HRRs and more fuels consumed. Therefore, activation time plays a key role in the system performance. However, the default low pressure system effectively suppressed the wood crib fire even with a late activation (i.e., a higher activation temperature), and thus the influence of late activation is limited. These results are in line with the large scale tests by Ingason et al. in 2013 [14] where the delayed activation time with a low pressure system was successively increased from 2 min to 4 min, and finally up to 8 min, and the activation heat release rate increased from 10 MW to 20 MW, but the system did not have any noticeable problem in controlling or suppressing the fire. The significant differences in the performance of various systems indicate that to effectively suppress loosely packed wood crib fires, adequate water densities are required.

4.3. Wood and HDPE crib fires with the top cover

4.3.1. Free-burn test

The results from the free burn wood and HDPE crib fire test are shown in Fig. 21 (the black line). The fire develops very rapidly, similar to the wood crib fire. The HRR reaches its peak value of 7.5 MW at 5.6 min, and then it dropped to around 6 MW for about 4 min before the

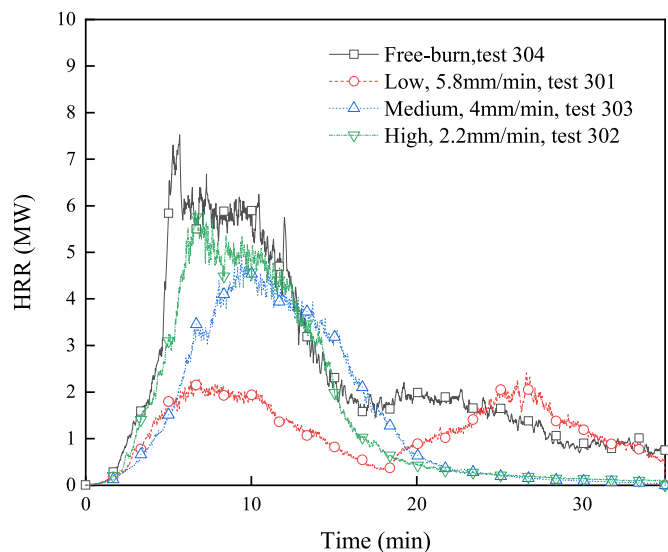


Fig. 21. HRRs in wood and plastic crib tests with various FFFSs and the top cover. Data from the free-burn test is plotted for comparison.

rapid decay. The maximum HRR is also slightly lower than the previous estimate of 8.4 MW. This should be related to the use of upper limit for wood as stated in Section 4.2. If 165 kW/m^2 is used for heat release rate per unit area of wood, the heat release rate becomes 7.7 MW, much closer to the measured value of 7.5 MW. The contribution from the HDPE to the HRR is rather significant. Although the volume portion of HDPE is only 14%, its contribution to the total HRR is estimated to be as high as about 50 %.

4.3.2. Comparison of default FFFSs with top cover

The results for the three default FFFSs with the top cover at 1.8 m/s is shown in Fig. 21. The activation HRR is around 0.5 MW at approx. 3 min. Clearly, the default low pressure system performs much better than the other systems, and the maximum HRR was 2.4 MW. By contrast, the HRR curve for the high pressure system is close to a free burn test, and it reaches the maximum value of 5.9 MW at 6.6 min. The medium pressure system does not perform well although it is slightly better than the high pressure system, and the fire reaches the maximum HRR of 4.9 MW at 9.3 min. The results for the energy released show less differences. From Table 3, the proportion of energy released is 55%, 61%, and 68% for the default low, medium and high pressure systems, respectively. For the default low and medium pressure systems, the fires had no impact on the targets, however, for the default high pressure system, the targets 1 to 3 were partially burnt and the other three were charred.

In general, the results are consistent with those for the wood crib fires. Due to the presence of the plastics (HDPE), complete suppression of the fire becomes more difficult as for plastics a higher water density is required for effective suppression, compared to wood [38]. The water densities used for the default medium and high pressure systems seem to be insufficient. Even for the low pressure system, the fire decays to around 0.5 MW at 18 min but it redevelops and reaches a second peak at around 27 min. From the visual observations during the test, the upstream part of the fuel was almost burnt out at 18 min.

To sum up, for both loosely packed wood crib fires, and wood and HDPE crib fires, the suppression performance seems to be proportional to the applied water density, and adequate water densities are required for effective suppression. The lower performance of the high pressure system is likely to be related to the weakened dilution effect due to the relatively better ventilation inside the loosely packed fuels, as explained earlier.

4.4. Pool fires without the top cover

4.4.1. Free-burn test

The HRRs from the heptane pool fire tests with various FFFSs as well as the free burn test is shown in Fig. 22 (the black line). The maximum HRR in the free burn test is around 0.9 MW before 13 min, but it rises to about 1.4 MW within a very short period. This phenomenon has also been observed in previous tests, e.g. Ref. [30]. The reason could be that at the final stage of a pool fire, the fuel layer becomes thin, and due to enhanced heat transfer the whole layer of fuel is heated up to boil [30].

4.4.2. Comparison of default FFFSs

A comparison of the HRRs in the tests without the top cover is shown in Fig. 22, as well as the free burn test data. In all the FFFS tests, at the activation time (3.5 min), the HRR is around 0.75 MW. Note that due to a mistake, 35 L of fuel was used in the free burn test 404 while the volume was 25 L in the other tests. Despite this, the HRR curve from the free burn test is very close to those from the other tests. This indicates that the influence of the fuel amount on the initial fire development is insignificant for such thick fuel pools.

For the low and medium pressure systems, after the activation, the HRR decreases immediately to around 0.3 MW. Note that in the low pressure test 401, at 10.5 min, a technical problem occurred with the water supply, but the operating conditions were reestablished at 12.3 min. In other words, during this 1.8 min period, the suppression system

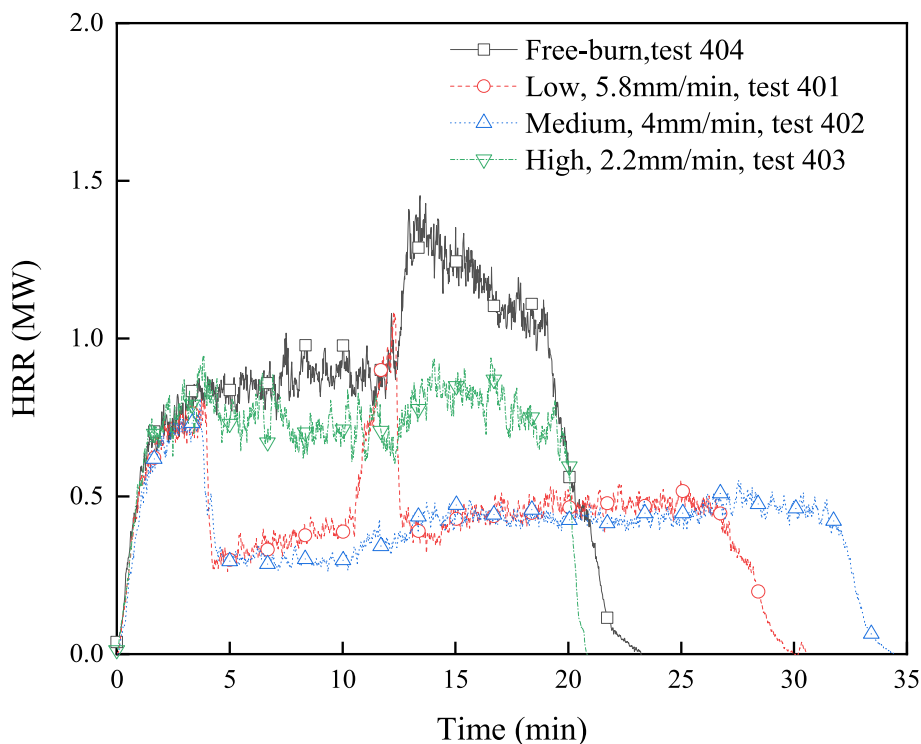


Fig. 22. HRRs in heptane pool fire tests with various FFFSs. Data from the free-burn test is plotted for comparison.

was not functioning, and no water was discharged. This can be seen from the HRR curve where the HRR rises to a higher level at around 12 min, close to the free-burn HRR. But shortly after the water supply is restored, the HRR drops to the same level before the system malfunction. The time for the suppression system to make full effect (period of the HRR decay) is approximately 30 s. This is much shorter than the time for the fire to restore its burning (period of the HRR increase), which is around 100 s. This phenomenon is positive from the fire protection point of view.

From Fig. 22 it can be observed that all of the FFFSs cannot extinguish the fire. For the low and medium pressure systems, the HRR increases slightly with the time after the system activation. This could be related to the continuous heating of the pan, surroundings, the fuel, and the water beneath the fuel. The sudden increase in the HRR at the final stage as can be found in the free burn test, however, does not occur for the low and medium pressure systems. This should be attributed to the fact that the thin fuel layer attached to the bottom of the pan as in the free burn test was not formed as there was always water left after these tests due to the water sprays continuously discharged to the pan. The HRR at the relatively stable level is around 0.45 MW. This indicates a reduction of 50% compared to the free burn HRR of 0.9 MW at the early stage or a reduction of 68% compared to the free burn HRR of 1.4 MW at the final stage. The similar performance of the low and medium systems could be explained by Heskestad's theory on extinction of gas and liquid pool fires with water spray [26] in an open environment. The medium pressure system has a lower flow rate but a higher operating pressure and momentum. This results in a smaller effective nozzle diameter and thus a lower critical water flow rate to extinguish a fire [26].

The HRR for the high pressure system is close to the free burn test. In contrast to the low and medium pressure systems, an increase of around 20% after 12 min can be observed, probably due to the lower water density applied for the high pressure system. This increase, however, is much lower than the increase of about 50% at the final state of the free burn test. Prior to 12 min, the HRR is about 0.75 MW, but afterwards it rises to about 0.9 MW. This indicates a reduction of 20% compared to the free burn HRR of 0.9 MW at the early stage or a reduction of 36% compared to the free burn HRR of 1.4 MW at the final stage. The

performance of the high pressure system cannot be well explained by Heskestad's theory in an open environment. The reason could be that in the test with the high pressure system, the influence of ventilation on the trajectories of water droplets cannot be ignored, different to an open environment. Significant amounts of water droplets may have been carried away by the air flow before reaching the pan, and thus the suppression effect could be much less than the other systems. As stated by Heskestad [26], it is much more difficult to suppress fires using fine-spray or misting nozzles in spaces where appreciable oxygen depletion cannot take place.

By visual observations during the tests, no fuel was spilled out of the pan. After each of the tests, no fuel but some water was left in the pan. The calculated energy released in the tests is also consistent with the amounts of fuel used. It can therefore be concluded that all the fuels were burnt out even in the presence of FFFS.

5. Conclusion

Fire suppression performance of various FFFSs, in terms of reducing the HRR and the total energy released, and preventing the fire spread to nearby vehicles, was investigated by carrying out several series of medium scale (1:3) tunnel fire tests. Three FFFSs were selected to represent typical systems used in road tunnels, namely a low pressure system, a medium pressure system and a high pressure system, referring to a water density of 10 mm/min, 6.8 mm/min and 3.7 mm/min, respectively in full scale. Other water densities were also tested to explore its effects, as well as the ventilation velocity and the activation criterion. Various fire scenarios were considered, i.e., wood pallet fires simulating densely packed fuels, wood crib fires and wood and plastic crib fires simulating loosely packed fuels, and heptane pool fires, with or without the top cover.

Comparisons of the three default systems based on the HRR, the total energy released and the possibility of fire spread to nearby targets show that the performance of the default low pressure system is usually the most effective in comparison to others in the densely packed fuel fires (without the top cover) and in all the loosely packed fuel fires (with or

without the top cover). For the densely packed fuel fires with the top cover, the three default system performs similarly but the low pressure system performs better at the early stage (before 12 min), and the medium pressure system performs better at the middle stage of the fire (between 12 min and 26 min). For the heptane pool fires, the low pressure and medium pressure systems perform similarly but significantly better than the high pressure system, and for both systems, the maximum HRR is reduced by 50%–68% of that in the free burn test, compared to 20%–36% for the high pressure system. Conclusively, in all the fire scenarios tested, the default low pressure system performs well and is usually the most effective, and the default high pressure system usually yields results less effective, using HRR, energy released and possibility of fire spread as measures. The performance of the default medium pressure system usually lies in between them, but in the idle wood pallet fires with the top cover, the performance during a certain period is slightly better than the low pressure system.

The high pressure system performs very differently in many aspects in comparison to the low and medium pressure systems. These aspects include tunnel ventilation velocity, water density, operating pressure, and the presence of the top cover. In both the idle wood pallet and wood crib fires, the influence of the fire source location on the suppression performance appears to be insignificant, but the top cover plays a key role in fire suppression. Without the top cover, the default low and medium pressure systems perform more efficiently than the scenario with the top cover. However, the default high pressure system performs slightly better in the wood pallet fire test with the top cover. In the wood pallet fires, for a given system, a reduction of the longitudinal ventilation velocity, or an increase in the water density improves the performance of the low and medium pressure system but has no or even negative effects on the performance of the high pressure system. This indicates that the suppression mechanisms of the high pressure system are different to the others, which does not rely on forceful penetration through the fire plume and direct surface cooling, but more on, e.g., gas cooling and dilution.

Comparisons of performance of different systems with same water densities but different operating pressures in the idle wood pallet fires with the top cover show that an increase of the operating pressure from the low pressure system level to the medium system level improves the fire suppression performance. But it is on the opposite side when the operating pressure is increased from the medium pressure system level to the high pressure system level. This indicates that, for the covered fires, there appears to be an optimal pressure between the low and high pressure systems, and probably between the low and medium pressure system levels due to the corresponding larger differences. In other words, a slight increase in the operating pressure of a low pressure system whilst applying the same water density may probably improve the system performance in the densely packed fires with the top cover. The system may perform equally well in the other scenarios due to the same water density applied. This provides a possible way to further improve the performance of the low pressure system.

In terms of preventing the fire spread to nearby targets, the low pressure system demonstrated good efficiency, and only in one test at the lowest water density of 4 mm/min was the first target charred. The medium pressure system also performs relatively well in preventing fire spread, with the first target being charred in only two tests. By contrast, the high pressure system was not as efficient in preventing the fire spread. In the majority of the tests with the high pressure system, one or more targets were partially burnt. Note that the results of fire spread should be considered as the combined effect of the amount of water delivered to the targets, and the heat exposed to the targets, which depends on the HRR, the ventilation velocity, and the gas cooling and radiation attenuation effects of the water droplets. Nevertheless, there appears to be a trend that a higher water density and larger droplet size facilitates the prevention of fire spread to downstream objects or vehicles, and the dependence of fire spread on the system pressure seems to be a secondary factor in these tests.

6. Limitations and future work

This work focuses on comparing the performances of different FFFSs in terms of reducing the HRR and the total energy released, and preventing the fire spread to nearby targets. The influence of the tested systems on gas temperature, gas concentration and visibility attenuation will be covered in a separate paper.

Most of the tests were carried out using the three default FFFSs. The default water densities for the medium and high pressure systems are close to or slightly greater than the commonly used values. It is expected that this may cause overestimations of the performances of the medium and high pressure systems in these tests.

The FFFS design is simple, i.e., two rows of ceiling mounted nozzles with downward sprays and an equal spacing for all the systems. In practice, a different design may affect the results, e.g., using side spraying nozzles like the ones used in the Runehammar tunnel fire tests [3, 14], having a lower tunnel clearance or a lower positioning of the nozzles.

Nowadays, alternative fuel vehicles are used in almost every type of transportation, e.g., car, bus, HGV and train locomotive, with various types of energy carriers: liquid fuels, liquefied fuels, compressed gases, and electricity [39]. Use of FFFS in tunnels could also benefit the increasing use of such vehicles, as a FFFS could suppress fires and may also cool down gaseous or liquefied tanks and battery packs, thus having great potential to minimize the risks of tank rupture and thermal runaway of batteries. The research on this topic is clearly needed.

CRediT authorship contribution statement

Ying Zhen Li: Conceptualization, Data curation, Formal analysis, Funding acquisition, Investigation, Methodology, Project administration, Resources, Writing – original draft. **Haukur Ingason:** Funding acquisition, Methodology, Resources, Writing – review & editing. **Magnus Arvidson:** Methodology, Writing – review & editing. **Michael Försth:** Funding acquisition, Methodology, Writing – review & editing.

Declaration of competing interest

The authors declare the following financial interests/personal relationships which may be considered as potential competing interests:

Y.Z. Li and H. Ingason are serving as guest editors for a special issue. However, they are not involved in the editorial review or the decision to publish this article.

Other authors declare that they have no known competing financial interests or personal relationships that could have appeared to influence the work reported in this paper.

Data availability

Data will be made available on request.

Acknowledgement

The work was financially supported by the Swedish Research Council Formas (2019-00521), which is gratefully acknowledged. The authors would also like to express their gratitude to Prof. Patrick van Hees at Lund University for his valuable input in the test planning process. Thanks also to our colleague Joel Blom, and other technicians at RISE for the great assistance in conducting the tests, and the Södra Älvsborg's Rescue Service for the support on site.

References

- [1] H. Ingason, Y.Z. Li, A. Löfnermark, *Tunnel Fire Dynamics*, Springer, New York, 2015.

- [2] U. Lundström, Development of the Swedish road tunnel safety concept, in: *Proceedings from the Tenth International Symposium on Tunnel Safety and Security*, 2023, pp. 45–55. Stavanger, Norway.
- [3] H. Ingason, Y.Z. Li, Large scale tunnel fire tests with different types of large droplet fixed fire fighting systems, *Fire Saf. J.* 107 (2019) 29–43.
- [4] Y.Z. Li, H. Ingason, Overview of research on fire safety in underground road and railway tunnels, *Tunn. Undergr. Space Technol.* 81 (2018) 568–589.
- [5] T. Lemaire, Y. Kenyon, Large Scale Fire Tests in the Second Benelux Tunnel, vol. 42, *Fire Technology*, 2006, pp. 329–350.
- [6] Development of new innovative technologies, UPTUN Work Package 2, 2006.
- [7] M. Tuomisaari, Full Scale fire testing for road tunnel applications - evaluation of acceptable fire protection performance, in: A. Lönnemark, H. Ingason (Eds.), *Third International Symposium on Tunnel Safety and Security*, 2008, pp. 181–193. Stockholm.
- [8] J.R. Mawhinney, Evaluating the performance of water mist systems in road tunnels, in: *IV Congreso Bienal Apci Ingenieria de Pci*, 2007. Madrid.
- [9] A.D. Lemaire, V.J.A. Meussen, Effects of Water Mist on Real Large Tunnel Fires: Experimental Determination of BLEVE-Risk and Tenability during Growth and Suppression, *Efectis Nederland BV*, 2008.
- [10] S. Kratzmeir, M. Lakkonen, Road Tunnel Protection by water mist systems - implementation of full scale fire test results into a real project, in: *Third International Symposium on Tunnel Safety and Security*, SP Technical Research Institute of Sweden, Stockholm, 2008.
- [11] SOLIT, Engineering Guidance for a comprehensive Evaluation of Tunnels with fixed fire fighting systems Scientific report of the SOLIT² research project, in: *Annex 3 - Engineering Guidance for Fixed Fire Fighting Systems in Tunnels*, 2012. The SOLIT² consortium.
- [12] M.K. Cheong, W.O. Cheong, K.W. Leong, A.D. Lemaire, L.M. Noordijk, Heat Release Rates of Heavy Goods Vehicle Fire in Tunnels with Fire Suppression System, *Fire Technology*, 2013.
- [13] M.K. Cheong, W.O. Cheong, K.W. Leong, A.D. Lemaire, L.M. Noordijk, F. Tarada, Heat release rates of heavy goods vehicle fires in tunnels, in: *15th International Symposium on Aerodynamics, Ventilation & Fire in Tunnels*, BHR Group, Barcelona, Spain, 2013.
- [14] H. Ingason, Y.Z. Li, G. Appel, U. Lundström, C. Becker, Large scale tunnel fire tests with large droplet water-based fixed fire fighting system, *Fire Technol.* 52 (5) (2016) 1539–1558.
- [15] C. Hue-Pei, H. San-Ping, C. Chao-Shi, C. Shen-Wen, Performance of a spray system in a full-scale tunnel fire test, *Tunn. Undergr. Space Technol.* 67 (2017) 167–174.
- [16] J. Li, Y.F. Li, Q. Bi, Y. Li, W.K. Chow, C.H. Cheng, C.W. To, C.L. Chow, Performance evaluation on fixed water-based firefighting system in suppressing large fire in urban tunnels, *Tunn. Undergr. Space Technol.* 84 (2019) 56–69.
- [17] L. Jiang, R.H. Mostad, T. Li, K.S. Arsava, Experimental study of the performance of a water mist system on fires in a full-scale tunnel, in: *Proceedings from the Tenth International Symposium on Tunnel Safety and Security*, RISE Research Institutes of Sweden, Stavanger, 2023.
- [18] H. Ingason, Model scale tunnel tests with water spray, *Fire Saf. J.* 43 (7) (2008) 512–528.
- [19] Y.Z. Li, H. Ingason, Model scale tunnel fire tests with automatic sprinkler, *Fire Saf. J.* 61 (2013) 298–313.
- [20] E. Blanchard, P. Boulet, P. Fromy, S. Desanghere, P. Carlotti, J.P. Vantelon, J. P. Garo, Experimental and numerical study of the interaction between water mist and fire in an intermediate test tunnel, *Fire Technol.* 50 (2014) 565–587.
- [21] Y.Z. Li, H. Ingason, Parametric study of design fires for tunnels with water-based fire suppression systems, *Fire Saf. J.* 120 (2021) 103107.
- [22] Y.Z. Li, H. Ingason, Influence of fire suppression on combustion products in tunnel fires, *Fire Saf. J.* 97 (2018) 96–110.
- [23] H. Ingason, Y.Z. Li, M. Arvidson, L. Jiang, Fire tests with automatic sprinklers in an intermediate scale tunnel, *Fire Saf. J.* 129 (2022) 103567.
- [24] NFPA 13 - Standard for the Installation of Sprinkler Systems, National Fire Protection Association, 2023.
- [25] NFPA 750 - Standard on Water Mist Fire Protection Systems, National Fire Protection Association, 2023.
- [26] G. Heskestad, Extinction of gas and liquid pool fires with water spray, *Fire Saf. J.* 38 (2003) 301–317.
- [27] M. Arvidson, Large-Scale Water Spray and Water Mist Fire Suppression System Tests for the Protection of Ro-Ro Cargo Decks on Ships, vol. 50, *Fire Technology*, 2014, pp. 589–610.
- [28] Y.Z. Li, H. Ingason, Scaling of wood pallet fires, *Fire Saf. J.* 88 (2017) 96–103.
- [29] P.A. Croce, Y. Xin, Scale modeling of quasi-steady wood crib fires in enclosures, *Fire Saf. J.* 40 (2005) 245–266.
- [30] Y.Z. Li, C.G. Fan, H. Ingason, A. Lönnemark, J. Ji, Effect of cross section and ventilation on heat release rates in tunnel fires, *Tunn. Undergr. Space Technol.* 51 (2016) 414–423.
- [31] H. Ingason, Y.Z. Li, A. Lönnemark, Runehamar tunnel fire tests, *Fire Saf. J.* 71 (2015) 134–149.
- [32] H. Ingason, A. Lönnemark, Heat release rates from heavy goods vehicle trailers in tunnels, *Fire Saf. J.* 40 (2005) 646–668.
- [33] M. Janssens, W.J. Parker, Oxygen consumption calorimetry, in: V. Babrauskas, T. J. Grayson (Eds.), *Heat Release in Fires*, E & FN Spon, London, UK, 1992, pp. 31–59.
- [34] B.Z. Dlugogorski, J.R. Mawhinney, V.H. Duc, The measurement of heat release rates by oxygen consumption calorimetry in fires under suppression, in: *Fire Safety Science - Proceedings of the Fourth International Symposium*, Ottawa, Canada: International Association for Fire Safety Science (IAFSS), 1994.
- [35] H. Ingason, Y.Z. Li, G. Appel, U. Lundström, C. Becker, Large Scale Tunnel Fire Tests with Large Droplet Water-Based Fixed Fire Fighting System, vol. 52, *Fire Technology*, 2016, pp. 1539–1558.
- [36] G. Rein, R. Carvel, J.L. Torero, Approximate trajectories of droplets from water mist suppression systems in tunnels, in: *Proceedings from the Third International Symposium on Tunnel Safety and Security*, SP Technical Research Institute of Sweden, Stockholm, Sweden, 2008.
- [37] Y.Z. Li, B. Lei, H. Ingason, The maximum temperature of buoyancy-driven smoke flow beneath the ceiling in tunnel fires, *Fire Saf. J.* 46 (4) (2011) 204–210.
- [38] H.-Z. Yu, J.L. Lee, H.-C. Kung, Suppression of rack-storage fires by water, in: *Fire Safety Science - Proceedings of the Fourth International Symposium*, 1994.
- [39] Y.Z. Li, Study of fire and explosion hazards of alternative fuel vehicles in tunnels, *Fire Saf. J.* 110 (2019) 102871.